Characterization of Proteins Released by Osteoblasts That Promote Expansion of Hematopoietic Progenitors

Owen Hovey

A thesis submitted in partial fulfillment of the requirements for the Master of Science in Immunology

Department of Biochemistry, Microbiology and Immunology
Faculty of Medicine
University of Ottawa

© Owen Hovey, Ottawa, Canada, 2018

Abstract

Umbilical cord blood (UCB) is a source of hematopoietic stem and progenitor cells (HSPC) used for allogeneic transplantation. *Ex vivo* expansion of HSPC can improve the slow platelet and neutrophil engraftment associated with UCB transplants. HSPCs reside in niches, some of which are near the endosteal bone surface, where they can associate with immature osteoblasts. Interestingly, osteoblasts can enhance the growth of HSPC in culture and their platelet engraftment activity. Using a proteomics approach, I identified 47 differentially expressed proteins between mesenchymal stem cells and immature osteoblasts. Several of these were previously implicated in HSPC maintenance such as IGF2, IGFBP2, DCN, GAS6 and VCAM1. Moreover, several other proteins belong to the alternative and classical complement pathways. Finally, I discovered that microvesicles found in osteoblast conditioned medium may also modulate the growth of HSPC, at least in *ex vivo* cultures.

Acknowledgments

I would first like to thank Canadian Blood Services for their funding and use of their facilities and for providing umbilical cord blood for this research. I would also like to thank my thesis supervisor Dr. Nicolas Pineault for his valuable guidance and support throughout the course of my master's degree. The opportunity afforded to me to work with mass spectrometry has been invaluable and has opened up new pathways in my life.

I would also like to thank all of the members of Dr. Pineault's Laboratory for their support and guidance. A thank you, to Roya Pasha and Matt Michalicka for teaching the techniques of the Pineault Laboratory. A thank you, to Dr. Javed Manesia for his assistance on developing some of the ideas that led to the final experiment in this thesis.

I would like to thank my family for all of their support through my degree helping whenever I needed the support. A very special thank you to Jim Gasper, a teacher who made a lasting impact on and got me to where I am today.

Lastly, I would like to thank my thesis advisory committee members, Dr. Daniel Figeys and Dr. Nadine Wiper-Bergeron for all of their suggestions and guidance though the many committee meetings

Table of Contents

List of Figures

List of Tables

List of Abbreviations

ABC — ammonium bicarbonate

ALP — Akaline phosphatase

BFU-E — Blast forming unit–Erythroid

BIT — BSA, Insulin and transferrin

BM — Bone Marrow

CFC — Colony forming cell

CFU-E — Colony forming unit-Erythroid

CFU-GM— Colony forming unit-granulocyte, macrophage

CFU-GEMM — Colony Forming Unit-granulocyte, erythroid, macrophage, megakaryocyte

CLP — Common lymphoid progenitors

CMP — Common myeloid progenitors

COMP — Cartilage oligomeric matrix protein

DCN — Decorin

DMEM — Dulbecco's Modified Eagle Medium

DTT — Dithiothreitol

FA — Formic Acid

FASP — filter aided sample preparation

FBS — Fetal bovine serum

GAS6 — Growth arrest-specific 6

HSC — Hematopoietic stem cells

HSPC — Hematopoietic stem and progenitor cells

IAA — Iodoacetamide

IGF1R — Insulin-like growth factor 1 Receptor

IGF2 — Insulin-like growth factor 2

IGFBP2 — Insulin-like growth factor 2

IGFBP4 — Insulin-like growth factor 4

IMDM — Iscove's Modified Dulbecco's Medium

kDa — Kilo Dalton

LGALS-3 — Galectin-3

LTC-IC — Long-term culture initiating cell assay

MEP — Common myeloid progenitors

MiQE — Minimum information for publication of quantitative real-time PCR experiments

Mk — Megakaryocytes

MPP — Multipotent progenitor

MS — Mass spectrometry

MS/MS — Tandem mass spectrometry

LC-MS/MS — Liquid Chromatography tandem mass spectrometry

OMPC — Optimized megakaryocyte progenitor cocktail

PBS — Phosphate Buffered Saline

qPCR — Quantitative Polymerase Chain Reaction

RT-qPCR — Reverse Transcription Quantitative Polymerase Chain Reaction

SCF — Stem cell factor

SPARC — secreted protein acidic and rich in cysteine

TNC — Total nucleated cells

TPO — Thrombopoietin

UCB — Umbilical Cord Blood

VCAM1 — Vascular cell adhesion protein 1

αMEM — Alpha-minimal essential medium

Chapter 1: Introduction

1.1 Hematopoietic stem cells and hemopoiesis

The cells within our blood are continuously being turned over throughout our lives through a hierarchical process known as hemopoiesis. Hematopoietic stem cells (HSC) are the source of all the different blood and immune cells through the process of hematopoiesis [1]. The two key properties of HSC are that they can self-renew and they can differentiate. The division of HSCs occurs either symmetrically, producing an identical progeny or asymmetrically, with one daughter cell similar to the mother and the other daughter cell committed to terminal differentiation [2]. The different markers for each lineage segregate to each side of the cell during asymmetric division [3]. The HSCs with greatest proliferative potential are those with the slowest growth kinetics [2]. The majority of HSCs reside within a quiescence state, G_0 phase of the cell cycle protecting the HSCs from exhaustion [4].

A transmembrane phosphoglycoprotein, CD34 has primarily defined human HSC characterization [5]. Cells enriched with this marker had colony forming potential [6]. Since the discovery of the CD34 marker, additional markers including the lack of CD38 and CD45RA expression, which are highly enriched with repopulating cells[7,8].

With HSCs at the apex, they differentiate down either the myeloid or lymphoid lineage [9]. While the lymphoid lineage leads to T, B and natural killer cells, the myeloid lineage leads to granulocytes (neutrophils, eosinophils, mast cells, and basophils), monocytes, erythrocytes, and megakaryocytes (Figure 1). HSCs differentiate in a stepwise manner down the lineage, and these stages can be characterized using

immunophenotyping. The “classical” model of hemopoiesis has multipotent progenitors (MPPs), with transient repopulation capacity a step before segregation of the lineages into common lymphoid progenitor (CLP) and common myeloid progenitor (CMP). However, recent findings have at times challenged this view, with recent studies suggesting that some lineage, like megakaryocyte, can be directly derived from HSC bypassing the common myeloid progenitor altogether, but this topic remains a controversial matter [10,11].

Most research on HSCs has been performed on murine models, these models allow for experimentation that could not be performed on humans [12]. Not all CD34+ cells have the potential to give rise to progenitors, the colony forming cell (CFC) assay is a method of determining the number of hematopoietic progenitors [13]. The CFC assay gives rise to colony forming cells of erythroid; burst forming unit-erythroid; granulocyte; macrophage; granulocyte; macrophage; granulocyte, erythrocyte; macrophage; megakaryocyte (CFC-E; BFU-E; CFU-G; CFU-M; CFU-GM; CFU-GEMM). Though a limitation of the CFC assay is not sufficient for detecting more immature or hematopoietic multipotent progenitor cells, these can be detected by a long-term culture-initiating cell (LTC-IC) assay. Transplantation study in immunodeficient xenograft murine models is the only model for assessing the HSC activity [12].

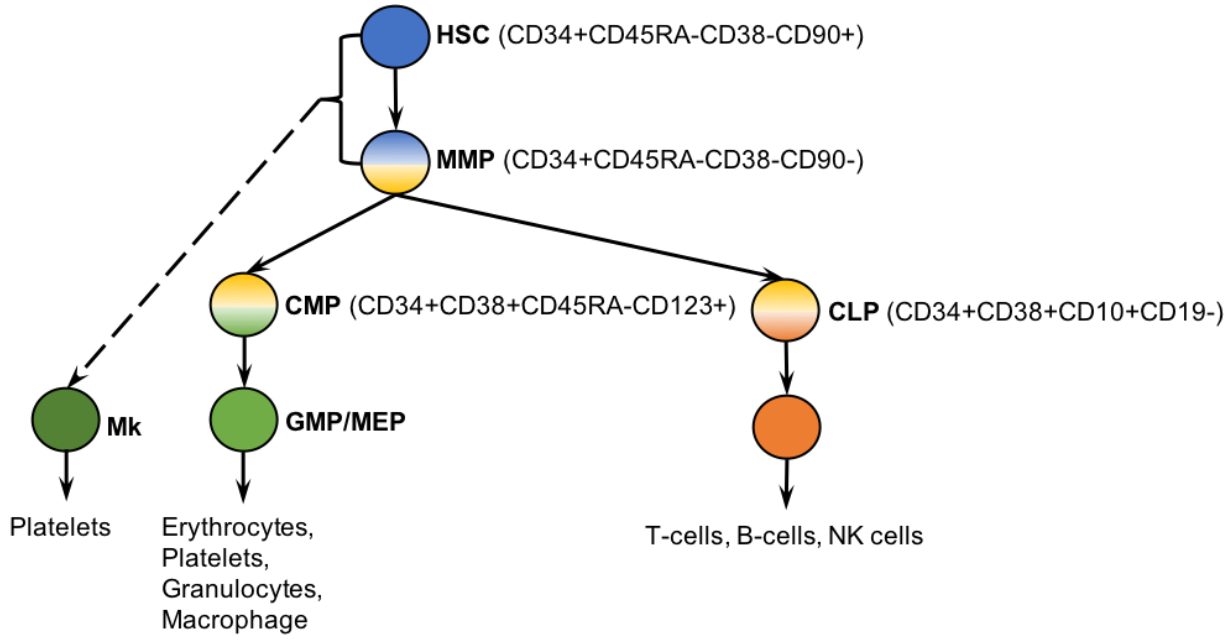

Figure 1: Overview of an evolving model of human hematopoietic hierarchy. The "classical" hematopoietic hierarchy shows hematopoietic stem cells (HSC) differentiating into the multipotent progenitor and then the lineage tree splitting into common myeloid progenitor (CMP) and common lymphoid progenitor (CLP). The CMP then further differentiates into the granulocyte-monocyte progenitor (GMP) and megakaryocyte-erythroid progenitor (MEP). Recent research suggests that megakaryocyte (Mk) bypasses the CMP from MPP and HSC populations, this represented by the dotted line [11].

1.2 Transplantation of Hematopoietic Cells and their Sources

In the 1950's hematopoietic cell transplantations were conceived as a way to treat irradiation, and by the end of the decade, successful treatment of end-stage leukemia was performed using identical twins bone marrow [14]. Since then the use of hematopoietic cell transplantations have been expanded to treat both malignant and non-malignant diseases including acute myeloid leukemia, non-Hodgkin's lymphoma, aplastic anemia, sickle cell anemia and more. Recently, a phase 2 clinical trial was completed using hematopoietic cell transplantations to treat aggressive multiple sclerosis[15]. With over 868 hematopoietic cell transplantation clinical trials currently in progress (clinicaltrials.gov) demand and uses for HSCs are likely to increase in the future.

Hematopoietic cell transplantations are either categorized as autologous, using the recipient's cells or allogeneic, using cells from a donor [16]. Hematopoietic cells for allogeneic transplantations have multiple options for sources to obtain the hematopoietic cells for transplant, which include bone marrow, mobilized peripheral blood and umbilical cord blood (UCB). UCB has the highest proportion of HSCs with 1 in 9.3×10^5 repopulating the bone marrow, while bone marrow and mobilized peripheral blood have 1 in 3.0×10^6 and 1 in 6.0×10^6 repopulating cells [17]. Only 30% of allogeneic hematopoietic cell transplants have a matched relative available [18]. About 60% of Caucasian recipients can find an unrelated matching donor while other ethnicities are less successful at finding a matching unrelated donor 20%-45%.

UCB transplants have many advantages compared to that of bone marrow and mobilized peripheral blood. These advantages include the ease of collection, minimal

risk to the donor, reduced wait times, a decrease human leukocyte antigen matching requirement and a reduced graft-*versus*-host disease occurrence [18]. These advantages do come with some drawbacks, which include limited cell dose per unit and a delayed neutrophil and platelet recovery. To combat the limited cell dose, double UCB transplantation was first successfully done in 2001[19], which improved engraftment in adult patients [20]. Though double UCB transplant increases recovery of neutrophil and platelet recovery, it is not comparable to mobilized blood, or bone marrow transplantations [21] and an increased occurrence of grade II graft-*versus*-host disease occurs [22]. The first UCBtransplantation happened in 1988 [23], since then the number of transplantations worldwide has grown to more than 25,000 worldwide with over 500,000 UCB units stored worldwide [18].

1.3 *Ex vivo* Expansion of HSCs

Multiple approaches for *ex vivo* expanding HSCs have been developed, as a method of solving the limited cell dose within a single UCB unit. Greater doses of HSCs produced by *ex vivo* expansion, lead to faster and maintained engraftment [24]. A larger dose of hematopoietic cells is preferable over transplantation with double UCB units, as there is a reduced unit requirement. Some methods developed so far for *ex vivo* expansion include the use of small molecule inhibitors, recombinant signalling molecules and, coculture and conditioned media from feeder cells [1]. Multiple signals regulate the balance between quiescence, self-renewal, differentiation, apoptosis and migration of HSCs. Stem cell factor (SCF), FMS-like tyrosine kinase 3 ligand (Flt-3L) and thrombopoietin (TPO) are important early acting cytokines involved in

hematopoietic stem and progenitor cell (HSPC) maintenance and combinations of them have been optimized to expanded HSPCs [25].

Differences such as oxygen content, supporting cells and nutrient content between the cell culture and the bone marrow microenvironment, causes difficulties in the maintenance of HSCs in cell culture [26]. Many signalling factors that regulate the growth of HSPCs have been identified using coculture and conditioned media from different cells types, from within the stem cells niche [27].

Ex vivo expansion of UCB using aryl hydrocarbon antagonist, StemRegenin-1 recently completed a Phase I/II clinical trial [28]. *Ex vivo* expansion with StemRegenin-1 improved neutrophil recovery to a median of 15 days compared to the control at a median of 24 days. Platelet recovery was also improved, with recovery at a median of 49 days compared to a median of 89 days. Additional clinical trials have been completed using coculture, NiCord technology and StemEx [27].

1.4 The stem cell niche within the bone marrow

The bone marrows' microenvironment contains multiple different cell types that regulate HSCs such as osteoblasts, mesenchymal stem/stromal cells (MSC), perivascular cells, adipocytes and endothelial cells. This microenvironment regulates self-renewal, differentiation and quiescence of the HSCs [26]. The different locations of HSPCs within the bone marrow microenvironment regulate the differentiation and proliferative abilities. There have been two proposed niches for HSCs, the endosteal niche which is the bone surface and the vascular niche, associated with blood vesicles.

The HSC niche is primarily associated with perivascular tissue which is made up of MSCs and endothelial cells but there is controversy about the HSC niche's proximity

to the endosteal surface[29]. This issue stems from the rarity of the HSC. Multiple studies have now imaged the bone marrow niche to assess the true niche of HSCs [30]. A three-dimensional imaging of bone marrow has shown that a higher proportion (≈80%) of HSCs are within 50% of the distance to the endosteal surface [31]. Though the majority of HSCs may be closer to the endosteal surface than the central vein, the physical association of HSCs was not statistically significant compared to that of other cell types. 90% of osteoblasts were either adjacent or in proximity to vasculature where the HSPCs were observed using live animal imaging [32]. The proximity but lack of association indicates that HSPCs associate with the endothelial cells of the vasculature and are likely susceptible to paracrine signalling from the osteoblasts. Recently, with improved markers for HSC markers both dividing and non-dividing HSCs were found to be distant from both the arterioles and endosteal surface and primarily near perisinusoidal tissue [30].

Initially, post-transplantation HSPCs were further away from the endosteal surface but as weeks progressed their proximity increased. Additionally, as cells became more differentiated their proximity increased from the endosteal surface. A gradient of secreted factors and extracellular matrix from osteoblasts was proposed by Lo Celse et al. to regulate the stem cell function. The maintenance of HSCs requires intermediate (CD146+) and mature (CD166+) osteoprogenitors [33].

Adipocyte, fat storage cells, differentiation within the bone marrow microenvironment increases with age and obesity [34]. Obesity leads to deficits in immune system development, which is attributable to the increase in adipocytes in the bone marrow niche. The shift toward adiposity leads to hematopoietic development shifting

towards the myeloid lineage over lymphocyte lineage, leading to reduced B-cell and T-cell numbers [35]. Factors such as adiponectin inhibit the development of B-cells. Soluble factors from early adipocyte also lead to an increase in myeloid lineage CD14+ cells [36]. Inhibition of adipogenesis in donor recipients leads to improved reconstitution of HSCs [37]. Hematopoietic deficiencies from increases in adiposity are attributable to the reduction in MSCs and their shift away from osteogenesis.

CXCL12 and SCF, which are critical cytokines for regulation of HSCs, were conditionally deleted from different cell types within the stem cell niche [38,39]. The conditional deletions of SCF show that perivascular and endothelial cells are critical regulators of HSCs, while osteoblasts marked by Col2.3-Cre were shown not to be the vital source of SCF for HSC [39]. In a similar study conditionally deleting CXCL12 indicated that reticular cells around the sinusoids are critical for maintenance [38]. Deletion of CXCL12 in osteoblasts again using Col2.3-Cre did not have any effect on the maintenance of HSCs, although the deletion of CXCL12 in osteoblasts did show a reduction in levels of early lymphoid progenitors and, B and T Cells. Altogether, the most recent studies point to the vascular niche being the most important for HSC maintenance and regulation under steady state hematopoiesis.

1.5 Mesenchymal stem/stromal cells

MSCs are also known as mesenchymal stromal cells and multipotent stromal cells in the literature [40]. First discovered in the early 1970's, these are highly adherent cells found within populations of hematopoietic cells from the bone marrow [41]. Researchers have also discovered MSCs in several other tissues, including adipose tissue and UCB [42,43]. MSCs have been defined by the International Society for Cellular

Therapies using three criteria [44]. These are firstly the ability to differentiate into osteoblasts, chondrocytes and adipocytes, secondly the absence of hemopoietic markers and the presence of CD73, CD90, CD105, and lastly the adherence to plastic. MSCs have three primary functions for therapeutic use, and these include tissue replacement through differentiation; immunomodulatory and anti-inflammatory effects; and paracrine tissue repair [40].

MSCs have been used to *ex vivo* expand HSCs in multiple studies, now using either coculture or conditioned media models [45–48]. Co-transplantation of MSCs with HSCs has been shown to reduce the occurrence of graft-versus-host disease and transplant-related mortalities [49]. Researchers have completed a phase 1 clinical trial for *ex vivo* expansion of HSCs using coculture with MSCs[50]. An improvement in neutrophil engraftment with a median of 15 days from the coculture expanded UCB patients, compared to a median of 24 days for the patients receiving unmanipulated units. An improvement was also seen in platelet engraftment, with a median of 42 days before platelet recovery for the coculture expanded unit, compared with the unmanipulated control at 49 days.

1.6 Osteoblasts and their differentiation

The bone is involved in vital processes, including mechanical support, locomotion and mineral homeostasis [51]. The bone is composed of 10% cells, 60% hydroxyapatite and 30% organic matrix, which is primarily composed of type 1 collagen. Osteoblasts, mineral depositing cells, and osteoclasts, mineral reabsorbing cells, regulate the composition of the bone matrix [52]. Through signalling of RANK and M-CSF from osteoblasts and MSCs, macrophages are differentiated into osteoclasts. [51].

Osteogenesis of MSCs differentiates into osteoblasts by signalling from paracrine and autocrine sources of Wingless-ints (Wnt), bone morphogenetic proteins (BMP) and insulin-like growth factors (IGF) [52,53]. These signalling factors lead to activation of RUNX2 and osterix, transcription factors involved in osteoblast differentiation. Initiation of osteogenesis begins with the activation of SOX9, which restricts MSCs to either the chondrocyte's or osteoblast's lineage [54]. The activation of SOX9 leads to the activation of the downstream transcription factor RUNX2 and at this point the MSCs are considered preosteoblasts. Canonical Wnt and BMP2/4 signalling also promote the signalling of RUNX2. Vitamin D promotes osteogenesis through both direct binding RUNX2 and histone deacetylation [55].

During the first stage of differentiation, preosteoblasts continue to proliferate and start to express osteonectin, collagen, TGFβ receptor 1, and osteopontin [55]. Increased secretion of ALP and collagen into the extracellular matrix and a halt in proliferation occurs during the second stage of differentiation. During the final stage of osteogenesis, an increase in the secretion of osteocalcin leads to the promotion of mineral deposits.

Our study uses chemically induced osteogenic differentiation using a combination of dexamethasone, ascorbic acid and β-glycerophosphate to stimulate differentiation in MSCs. Dexamethasone binds to the glucocorticoid response element which promotes the transcription of FHL2, a binding partner of β-catenin, which in turn leads to RUNX2 transcription [56]. Additionally, there is an upregulation of MKP-1 which promotes dephosphorylation of RUNX2, leading to enhanced transactivation. Ascorbic acid promotes the translocation of NFE2L1 into the nucleus, where it transcribes osterix

[57]. While β-glycerophosphate acts as a source of phosphate to produce hydroxylapatite minerals [56].

Ex vivo expansion using osteoblasts has been attempted using both conditioned media and co-culture models, showing increased production of HSPCs [45]. Primary osteoblasts in co-culture induce expansion of CD34+ and CD34+CD41+ [58]. Contact culture of CD34+Lin- cells with primary osteoblast promote the expansion of colony forming cells, but the removal of contact eliminates this effect. In non-contact cultures, the addition of the ligands for LFA-1, ICAM-1 and/or the ligand for VLA-4, either FN1 or VCAM-1 can restore the expansion of colony forming cells [59]. These factors FN1, ICAM-1 and VCAM-1, require additional unknown factors secreted by osteoblasts. Additionally, expansion of HSPCs in coculture with primary osteoblasts is correlated with RUNX2 expression and inversely correlated with alkaline phosphatase activity and mineral deposition[60].

Ex vivo expansion using osteoblasts in one model was shown to be CXCL12 dependent, though our model shows the opposite trend in CXCL12 expression, indicating this may be specific to their model [61](Pineault, Unpublished). Additionally, decellularized matrix differentiated osteoblasts promoted the expansion of HSPCs, indicating that either matrix proteins or proteins stored in the extracellular matrix are involved in the expansion of HSPCs [62].

1.7 Extracellular Vesicles

Extracellular vesicles is an overarching term covering exosomes, microvesicles and apoptotic bodies [63] The lower range of size for exosomes varies depending on the study, but the upper limit is 100nm, while microvesicles are between 100-1000nm and

apoptotic bodies greater than 1000nm [63–65]. The assembly of exosomes and microvesicles are similar, though the release of exosomes and microvesicles is where the majority of the biogenesis of these extracellular vesicles differ [63]. Exosomes are released when multivesicular bodies fuse with the plasma membrane and release their exosomal contents. The storage of exosomes after biogenesis in multivesicular bodies allows for the controlled and timed release of the exosomes. Budding of the plasma membrane produces microvesicles through a vSNARE related mechanism. Characteristics such as size, zeta potential and composition of microvesicles are dependent on the culture conditions used to generate the microvesicles [66]. Microvesicles contain various cargo, including proteins, miRNAs and mRNAs. Microvesicles enriched with miRNAs regulating transcription factors, known to be involved in hemopoiesis from MSCs, leading to the expansion of CD34+ UCB cells [67].

There are few studies of microvesicles derived from osteoblasts. The addition of parathyroid hormone to the osteoblasts doubles the number of microvesicles that osteoblasts produce [68]. Parathyroid hormone also increased the amount of RANKL on the surface of the microvesicles secreted from the osteoblasts, changing their composition. Microvesicles from immortalized osteoblasts stimulated differentiation of RAW264.7 cells into osteoclasts. Additionally, osteoblasts have another extracellular vesicle type, which overlaps microvesicle definition, known as matrix vesicles. The matrix vesicles are between 100-300nm and produced through membrane budding [69]. Matrix vesicles are usually in the extracellular matrix bound to collagen. What separates the microvesicles from the matrix vesicles is that the matrix vesicles have extracellular matrix forming properties. Matrix vesicle characterization typically includes testing of

Alkaline phosphatase activity [70]. The addition of collagenases before collection has been shown to increase the yields of matrix vesicle during isolation.

1.8 Previous work using osteoblasts for *ex vivo* expansion of hematopoietic stem cells by the Pineault group

Previous work by the Pineault group showed that irradiation of MSCs observed increases in calcium deposits and osteopontin expression, markers that are typically associated with osteogenic differentiation [71]. These irradiated MSCs improved the production of megakaryocyte and total colony forming cells, prompting the evaluation of osteoblasts derived from MSCs as feeder cells for the *ex vivo* expansion of HSPCs [45].a Coculture without contact with osteoblasts recapitulated these effects. The condition that showed greater expansion in total nucleated, CD34+ and colony forming cells was media conditioned with osteoblasts compared to media conditioned with MSCs or non-conditioned media. Besides increasing CD34+ populations, the CD11b+ and CD14+ populations also observed a significant increase in expansion. Both these markers occur on multiple cell types, and further immunophenotyping should be performed to understand better the cell types promoted by osteoblast conditioned media. Initial characterization of osteoblast conditioned media showed upregulation of CXCL1, GM-CSF, IL7 and FGF7.

Expansion with osteoblast conditioned media was associated with a significant improvement in platelet engraftment in immunodeficient mice transplanting HSPCs expanded with osteoblast conditioned media over HSPCs expanded in serum-free media or with MSC conditioned media. The improvement in platelet engraftment using

osteoblast conditioned media started at the second week post-transplantation continuing through to four months in the majority of the time points. Indicating that osteoblast conditioned media presents a potential method that can be used to overcome delayed platelet recovery in UCB transplantation. Unknown factors secreted by osteoblasts that promote the increased cell proliferation and improved engraftment will be the focus of my thesis.

The osteoblast conditioned media was evaluated at different stages of osteoblast differentiation and this was investigated in the Pineault lab [72]. These results demonstrate that immature osteoblasts (day 6) promoted the greatest effects on multipotent and clonogenic hematopoietic progenitor cells. Osteoblast conditioned media increased the number of long-term culture initiating cells and colony forming cells, respectively. These results obtained with osteoblasts derived from human MSC are supported by results obtained with primary murine osteoblasts and further support the use of osteoblasts derived from human MSC as a model to study their implication as a regulator of HSC and progenitors [60].

Filtering (0.22μm) of the osteoblast conditioned media has been shown to abolish the effect of osteoblast conditioned media on the expansion of total nucleated cells [45]. Further characterization showed that filtering of osteoblast condition media primarily reduces growth-promoting effects on CD34+, CD34+CD45-, CD34+CD45RA-CD38- and colony forming cells [73]. The growth modulatory effect of osteoblast conditioned media on CD41+ and CD14+ populations was unaffected by the filtering process, indicating that the mechanism that regulates the growth of CD34+ population, and CD41+ and CD14+ from osteoblast conditioned media may be different. Filtering

osteoblast conditioned media lead to a reduction in platelet recovery, which is believed to be the result of the reduction in cell expansion (Abu-Khader, Manuscript Submitted).

1.9 Hypothesis and Objectives

Previous work in the Pineault laboratory has shown the potential of osteoblast conditioned media in expanding HSPCs with high thrombopoietic activity. This study aims to further characterize the secretome of immature osteoblasts, with biological relevance to the expansion of HSPCs and improving platelet engraftment. The hypothesis of this study stated that mass spectroscopy of osteoblast conditioned media would provide a means to identify soluble factors released by osteoblasts derived from human MSCs that may promote the growth of UCB progenitors. This project is broken up into three primary objectives.

The first objective was to identify a method that retained the growth modulatory activity of osteoblast conditioned media on HSCs while giving the greatest coverage of the secretome. Multiple methods were attempted to fractionate the conditioned media, altering the composition of the conditioning media and methods of conditioning. All of these methods were tested on HSPCs to test for growth modulatory effects, if the fractionated media retained the growth promoting activities of osteoblast conditioned media.

The second objective sought to quantitatively compare the secretome of MSCs and immature osteoblasts, using label-free mass spectrometry (MS). Using multiple bioinformatics techniques, quality and biological insights from the secretome data were evaluated to understand the data better.

The final objective was to validate secreted factors observed from the mass spectrometer data in early osteoblast differentiation. I validated multiple candidates from the MS by qPCR. I then tested two candidate proteins in CD34+ cell cultures and assessed the implication of extracellular vesicles in the growth modulatory activity of osteoblast conditioned media.

Chapter 2: Materials and Methods

2.1 Culture of human mesenchymal stem cells

hMSC lines (n=4) were previously isolated from independent bone marrow mononuclear cells in the Pineault laboratory (Lonza, Group Ltd, Basel, Switzerland). The HSPCs were previously characterized by Roya Pasha to meet the defined criteria of the International Society for Cellular Therapy [44]. HSPCs were cultured in alpha-minimal essential medium (Life Technologies, MA, USA) supplemented with 10% HyClone fetal bovine serum (FBS) (Fisher Scientific, Ottawa, Canada) in humidified atmosphere with 5% CO_2 at 37°C. Cells were passaged between 80-90% confluence using TryplE Select 1X (Life Technologies), and cell viability was checked by Trypan Blue Stain 0.4% (Life Technologies). Experiments used early passage HSPCs between 2-4. Four different bone marrow HSPC lines were used during this study.

2.2 Production of MSC-derived osteoblasts

Confluent HSPCs had their media replaced with alpha-minimal essential medium supplemented with 10% HyClone fetal bovine serum, 10^{-7} M dexamethasone (Sigma, St-Louis, MO, USA), 0.17 mM ascorbic acid (Sigma) and 10 mM β-glycerophosphate (Sigma). The media was replaced additionally on day 2 and 4 of differentiation.

2.3 Production of conditioned media

MSCs or M-OSTs were washed with phosphate buffered saline (PBS) five times and then replaced with 0.2mL/cm^2 of serum free media containing Iscove's modified Dulbecco medium (IMDM) supplemented with 20% BIT (BSA, insulin and transferrin) (StemCell Technologies, Vancouver, BC, Canada), 40 mg/ml of human low-density lipoproteins (LDL) (StemCell Technologies) and 5 x10^{-5} M β -mercaptoethanol (Sigma). The conditioned media was collected after 24 hours. For conditioned media, referred to as NO BIT, the 20% BIT 9500 supplement was omitted during the conditioning process and then re-added after. For conditioned media, referred to as CHASE, complete serum free media was added for 12 hours, then washed with PBS five times, and then replaced with serum free media omitting 20% BIT. The conditioned media was centrifuged after collection at 300xg for 6 minutes at room temperature. Conditioned media was aliquoted into 1.5mL cryotubes and stored at -80°C.

2.4 Isolation of CD34+ Cord Blood cells

The research described herein was approved beforehand by the Canadian Blood Services Research Ethical Board. Umbilical cord blood was provided by Canadian Blood Services after institutional review board approval and written informed consent from the mothers. Mononuclear cells from UCB were isolated using Lymphoprep^{TM} (StemCell Technologies). The CD34+ cells were isolated from mononuclear cells using EasySep^{TM} Human CD34 Positive selection kit (StemCell Technologies) according to manufacturer's protocol. Purity of each unit was assessed for greater than 90% using CD34 (Clone: 581) on Attune flow cytometer (Applied Biosystems by Thermo Fisher

Scientific, Waltham, MA, USA). The CD34+ selected cells were cryopreserved in 40% IMDM, 50% FBS and 10% DMSO at $1.0x10^5$ cells/mL

2.5 Expansion assay of CD34+

A combination of two UCB CD34+ –enriched cells were analyzed upon thawing to obtain percentage of each starting population and plated at 10,000 UCB cells/mL. Serum-free media, as previously described or conditioned media, was used supplemented with OMPC cocktail containing 10 ng/mL SCF, 35 ng/mL TPO and 11 ng/mL Flt3L (Peprotech, Rocky Hill, NJ, USA)[25]. Each condition was grown with two technical replicates in humidified atmosphere with 5% CO_2 at 37°C. On the fourth day of culturing one volume of fresh media was added. On day six of expansion a 100µl of culture volume was stained with antibodies for 20 minutes at room temperature and then diluted 1:5 and placed at 4°C until analysis. Samples were run on Attune flow cytometer (Applied Biosystems) with voltages set individually for each fluorophore stained on beads. The voltages were set at the inflection point of the negative peak's coefficient of variance (CV) with the highest stain index that remained on scale. Each lot antibody was titrated for optimal stain index.

Recombinant proteins LGALS-3 and SPARC (Novoprotein, Summit, USA) were centrifuged, reconstituted in distilled water and stored at -20°C. Recombinant proteins were diluted using PBS+0.1% BSA and added at either 10ng/ml or 20ng/ml to culture. Control wells had PBS+0.1% BSA added at an equal volume to the addition of recombinant protein. The expansion was calculated by dividing the starting number of

each population with expanded number on day 6. Each biological experiment used different UCB units.

Table 1: Antibody used for analysis of expanded umbilical cord blood CD34+.

Antigen	Company	Clone	Fluorophore
CD34	BD Biosciences	581	PE
CD38	BD Biosciences	HIT2	FITC
CD45RA	BD Biosciences	HI100	APC
CD90	BD Biosciences	5E10	PE-Cy7

2.6 FASP fractionation of conditioned media

Osteoblast conditioned media was concentrated using either 30kDa, 50kDa or 100kDa of filter aided sample preparation (FASP) spin columns centrifuged at 10,000g for 10 minutes (EMD Millipore, Darmstadt, Germany). Flow through from osteoblast conditioned media and serum free media had 20% BIT re-added and 40 mg/ml low-density lipoproteins. While retentate of osteoblast conditioned media and serum free media was diluted with IMDM back to the starting volume of 1.5ml. These media were then used in expansion assays of CD34+ as described above.

2.7 In-solution digestion and mass spectrometry acquisition

MSC conditioned media and osteoblast conditioned media (4.5 mL) from 4 cleaning independent MSC lines were concentrated using Amicon Ultra-4 3kDa centrifugal filter unit. Then 30μg was diluted 1:2 with 8M Urea (Sigma) in 50mM ammonium bicarbonate (ABC) (Sigma). Reduction and alkylation were done by adding DTT (Sigma) to a final concentration of 20 mM for 45min followed by 40mM IAA (Bio-Rad, Hemel Hamstead, UK) for 30 minutes, all at room temperature. The samples were then diluted 5-fold by adding 50mM ABC. Trypsin (ThermoFisher Scientific, San Jose, CA) was added to achieve a protein-enzyme ratio of 30:1. Digestion was performed at 37°C overnight, with continuous shaking. Digested peptides were then cleaned up using Pierce™ C18 Spin Columns (ThermoFisher Scientific) and dried down in SpeedVac. Dried peptides were reconstituted in 0.5% (v/v) FA.

All samples run on MS were performed by Dr. Zhibin Ning, Research Associate at uOttawa Proteomics Resource Center using high-performance liquid

chromatography-electrospray ionisation tandem mass spectrometry (HPLC-ESI-MS/MS). The system consisted of an Agilent 1100 micro-HPLC system (Agilent Technologies, Santa Clara, CA, USA) coupled with an LTQ-Orbitrap mass spectrometer (ThermoFisher) equipped with a nano-electrospray interface operated in positive ion mode. The mobile phases consisted of 0.1%(v/v) FA in water as buffer A and 0.1% (v/v) FA in acetonitrile as buffer B. Peptide separation was performed on a 75μm × 100 mm analytical column packed in-house with reverse phase Magic C18AQ resins (1.9μm; 120-Å pore size; Dr. Maisch GmbH, Ammerbuch, Germany). Briefly, the sample was loaded on the column using 98% buffer A at a flow rate of 1.5μL/min for 15min. Then, a gradient from 5% to 35% buffer B (20~50% for APols depletion test) was performed in 120 min at a flow rate of ~300nL/min obtained from splitting a 20 μL/min through a restrictor. The MS method consisted of one full MS scan from 300 to 1700 m/z followed by data-dependent MS/MS scan of the 5 most intense ions, with dynamic exclusion repeat count of 2, and repeat duration of 90 seconds. As well, for the experiments on the Orbitrap MS the full MS was performed in the Orbitrap analyzer with R = 60,000 defined at m/z 400, while the MS/MS analysis were performed in the LTQ. To improve the mass accuracy, all the measurements in the Orbitrap mass analyzer were performed with internal recalibration ("Lock Mass"). On the Orbitrap, the charge state rejection function was enabled, with single and "unassigned" charge states rejected.

2.8 Database search and analysis of secretome samples

The raw files generated by the LTQ-Orbitrap were processed and analyzed using MaxQuant, version 1.6.1.0 [74] using the UniProt protein FASTA database (2012, July

version), including commonly observed contaminants. The following parameters were used: cysteine carbamidomethylation was selected as fixed modification; methionine oxidation, protein N-terminal acetylation, and enzyme specificity was set to trypsin. Up to two missing cleavages of trypsin were allowed. Precursor ion mass tolerances were 7 ppm, and fragment ion mass tolerance was 0.8 Da for MS/MS spectra. If the identified peptide sequences from one protein were equal to or contained within another protein's peptide set, then the proteins were grouped together and reported as one protein group. The false discovery rate (FDR) for peptide and protein was set at 1% and a minimum length of six amino acids was used for peptide identification. Quantification was performed using normalized LFQ intensity [75].

The LFQ intensity were analyzed using Perseus version 1.6.0.7 [76]. Targets labeled for "only identified by site", reverse or contaminant were excluded from analysis. Proteins with valid values in less than three out of four samples in either of the conditions were excluded. After filtering samples were normalized by the sum and transformed by $\log_2$. Imputation of missing values were calculated from a normal distribution using a width of 0.3 and downshift of 1.8. Correlations between samples were compared by using multi-scatter plots and Pearson's correlation. The samples were then compared using the principle analysis function within Perseus, component 1 through 7 were compared and then graphed in Prism. The two conditions were compared using a paired two-tailed student's t-test with a S_0 of 1 and a permutation-based FDR <0.05 with 250 randomizations.

2.9 Bioinformatics: Gene ontology enrichment and extracellular vesicles database comparison

Proteins upregulated during osteoblast differentiation were evaluated using gene ontology enrichment using FunRich [77] using the Uniprot database (March, 2018). Enrichment with a q-value greater than 0.05 using Storey-Tibshirani method was presented. Proteins observed with valid values in 3 out of the 4 biological replicates and upregulated proteins during differentiation were compared with the Vesiclepedia database of microvesicles and exosomes using FunRich [78] (March, 2018).

2.10 Depletion, isolation and characterization of microvesicles

Osteoblast conditioned media was centrifuged at 20,000g for 30 minutes at 4°C twice. After each centrifugation the supernatant was transferred to a new tube. The supernatant was then used in the CD34+ expansion assay as described above.

For isolation of microvesicles, osteoblast condition media was centrifuged at 1000xg for 10 minutes and then transferred to a new tube. Next supernatant was centrifuged at 20,000xg for 20 minutes at 4°C and then washed with one volume of PBS. The pellet was resuspended in PBS and sizing of extracellular vesicles was performed using nanoparticle tracking analysis using the Zetaview ® (Inning am Ammersee, Germany). Video was taken at 15 fps using 11 frames and 2 cycles.

Isolated microvesicles were spun down and resuspended in Annexin Binding buffer (ThermoFisher Scientific) and staining with Annexin V-AlexaFlour488 (ThermoFisher Scientific) and CD106 (VCAM-1) (BD biosciences) for 30 minutes at 4°C. After staining samples were then centrifuged down and resuspended in 500uL of

Annexin Binding buffer. Microvesicles were then analyzed on the Attune flow cytometer. A serum free control was used to set the gating for the microvesicles.

2.11 Quantitative reverse transcription polymerase chain reaction (RT-qPCR)

Isolation of confluent HSPCs and day 6 osteoblasts RNA was performed using Aurum™ Total RNA Mini Kit (BioRad, Hercules, CA, USA). RNA concentration and purity were determined using Bio Drop spetrophotometer (Montreal Biotech Inc., Kirkland, QC, Canada). RNA integrity was assessed by 28S/18S bands on 2% agarose gel. Samples with degraded RNA profiles were excluded. Synthesis of cDNA was performed using iScript™ Reverse Transcription Supermix with 1µg of RNA following the manufacture's protocol version C using CFX96 Touch™ Real-Time PCR Detection System (BioRad, Hemel Hamstead, UK). Primers were designed using NCBI primer-BLAST and theoretical values were also evaluated on IDT OligoAnalyzer 3.1. Once the primer with the best theoretical valueswas found the primer was ordered from IDT (IDT, Coralville, USA). qPCR reactions were performed using 4µl diluted cDNA, 0.5µl of RVS and FWD primers, 0.5µl nuclease free water (Coralville, Iowa, USA), and 5µl Sso Advanced Universal Sybr Green Supermix (BioRad). Pooled samples diluted 1:32 were used to assess optimal annealing temperature on a temperature gradient. Using the Ct values from the temperature gradient, the dilution series for the standard curve with the largest dynamic range was selected. Samples were diluted to the middle of the standard curve for analysis.

Quantification of each gene on each sample was done in three technical replicates using the following protocol on a CFX96 Touch™ Real-Time PCR Detection System: 95°C/3 min, followed by 40 cycles of 95°C/10 sec, (optimized temperature)/20 sec, 72°C/20 sec and melt curve analysis of 95°C/10 sec, 65°C/5 sec, 95°C/5s. Data was analyzed using the CFX Manager 3.1 software (BioRad). Using GeNorm five reference genes were compared and RPL13a, RPLP0, TBP and HPRT1 were selected as stable. All experiments and analysis was done in compliance with MIQE guidelines [79].

Table 2: Oligonucleotide primers designed for the site directed mutagenesis

Gene	Species		Primer	Amplicon Length	Accession number
C1R	Human	FWD	TTCCCCAAGCCTTACCCCAA	85	NM_001354346.1
		RVS	GCTGGAAGACGAGCTTCACC		
C1S	Human	FWD	TTTGGCATGGGTTTATGCTGA	140	NM_201442.3, NM_001734.4
		RVS	GGGTGAAGTAGAGGTGAATCCC		
C3	Human	FWD	TGTGAGCCAGGAGTGGACTA	114	NM_000064.3
		RVS	ATCCGAGCCTGACTTGATGG		
CD109	Human	FWD	GAAGCCATCTCTCAACTTCACA	146	NM_133493.4, NM_001159587.2, NM_001159588.2
		RVS	TTCCACTGTTAGATCCGCTCC		
CFD	Human	FWD	GATGTGCGCGGAGAGCAAT	171	NM_001928.3, NM_001317335.1
		RVS	CTGTCGATCCAGGCCGCATA		
CFH	Human	FWD	TACTGGCTGGATACCTGCTC	165	NM_000186.3, NM_001014975.2
		RVS	CCTGACGGAGTCTCAAAATG		
COMP	Human	FWD	AACAGTGCCCAGGAGGAC	191	NM_000095.2
		RVS	TTGTCTACCACCTTGTCTGC		
DCN	Human	FWD	GCCAACACGCCTCATCT	188	NM_001920.4, NM_133503.3, NM_133504.3, NM_133505.3
		RVS	CTCACACCCGAATAAGAAGCC		
GAS6	Human	FWD	GCCTTTCAGGTCTTCGAGGAG	210	NM_000820.3
		RVS	GTCAGGCAGGTTTTGCACG		
IGFBP4	Human	FWD	GTCACAGCCATGAAGTCACC	146	NM_001552.2
		RVS	CATCCAGTCAAGCCAGAAGA		
LOXL2	Human	FWD	CGGAGGATGTCGGTGTGGT	141	NM_002318.2
		RVS	GCTTGCGGTAGGTTGAGAGG		
WNT3a	Human	FWD	CAGGAACTACGTGGAGATCA	159	NM_033131.3
		RVS	GACTCCCTGGTAGCTTTGT		
WNT4	Human	FWD	TGTGACAGGACAGTGCATGG	75	NM_030761.4
		RVS	ACCGTAGGCGATGTTGTCAG		
WNT5a	Human	FWD	GCTCCGCTCGGATTCCTC	87	NM_003392.4
		RVS	CCAATGGACTTCTTCATGGCG		
Reference Genes					
GAPDH	Human	FWD	TCGACAGTCAGCCGCATCTTCTTT	94/186	NM_002046.6, NM_001357943.1, NM_001289745.2
		RVS	ACCAAATCCGTTGACTCCGACCTT		
HPRT1	Human	FWD	GACCAGTCAACAGGGGACAT	132	NM_000194.2
		RVS	CCTGACCAAGGAAAGCAAAG		
RPL13a	Human	FWD	TCAAGGTCGTGCGTCTGAA	171	NM_012423.3, NM_001270491.1
		RVS	CCTGTTTCCGTAGCCTCATG		
RPLP0	Human	FWD	CGTCCTCGTGGAAGTGACAT	176	NM_001002.3
		RVS	CTTGGAGCCCACATTGTCTG		
TBP	Human	FWD	GGCACCACTCCACTGTATCC	179	NM_003194.4, NM_001172085.1
		RVS	TTATATTCGGCGTTTCGGGC		

2.12 Statistical Analysis

Statistical analysis was performed using GraphPad Prism version 6.0e unless otherwise stated (La Jolla, CA, USA). Multiple group comparison was done using repeated measure one-way ANOVA with post-hoc test Tukey test. While comparison of two groups were done with a paired student's t-test. Comparisons with p-values less than 0.05 were considered to be significant

Chapter 3: Results

3.1 Osteoblast conditioned media fractionated by filter-aided sample preparation columns

The use of MS to identify proteins secreted by osteoblasts requires a minimal background from the medium used in the conditioning process to observe as deep as possible into the secretome. The presence of serum components such as albumin reduces the dynamic range of the mass spectrometer and thereby reduces the number of identified proteins [80]. A method for producing conditioned media that retained the growth modulating activity of osteoblast conditioned media and a minimal background had to be identified to examine changes in protein secreted from HSPCs to immature osteoblasts (day 6). The first method attempted, was to fractionate the osteoblast conditioned media above and below, 30kDa, 50kDa and 100kDa using filter-aided sample preparation (FASP) columns.

The unfractionated osteoblast conditioned media for the 50kDa and 100kDa experiments showed a significant increase in the expansion of both total nucleated cells (>2.7-fold, $p<0.0001$, Figure 2C & E) and CD34+ cells (>2.1-fold, $p<0.001$, Figure 2D & F) compared to control serum-free media replicating our group's previous results. The unfractionated osteoblast conditioned media samples with the 30kDa experiments also increased expansion, though not significantly due to high variation between experiments (Figure 2A & B). Expansion of total nucleated cells in the retentate fraction induced a significant increase in all three FASP columns (2.8-fold, $p=0.0099$; 2.3-fold, $p=0.011$; 1.4-fold $p=0.03$, respectively) (Figure 2A, 1C, 1E) suggesting that secreted factors responsible for total nucleated expansion are either too large or in complexes too large

to pass through the 100kDa FASP column. Expansion of CD34+ population increased for each of the three FASP column sizes, but the increases were not significant (Figure 2B, D & F). The fold increases of the total nucleated cells and CD34+ cells have a decreasing trend as the size of the FASP columns increased.

None of the flow through conditions from the three FASP column sizes induced a significant change in expansion and did not follow any discernible trends (Figure 2). In all of the FASP column size samples, there was a reduction in the expansion induced by the flow through of the serum-free media compared to the unfractionated serum-free media, though the decrease was only significant for the 100kDa columns ($p=0.012$; $p=0.0019$, respectively) (Figure 2E & F). This likely indicates that one or more components of the serum-free media are becoming trapped in the column filter. The fractions of osteoblast conditioned media containing the greatest promoting activity were the retentate of the 30kDa and 50kDa, which overlap with the fraction containing bovine serum albumin from the serum-free media (Figure 2A-D). Minimal activity in the retentate and flow through for the 100kDa was observed compared to the unfractionated, likely indicating that active components were trapped within the filter (Figure 2E & F). The abundance of bovine serum albumin in the media masked the presence of other targets in one MS attempt, ruling out the use of this method.

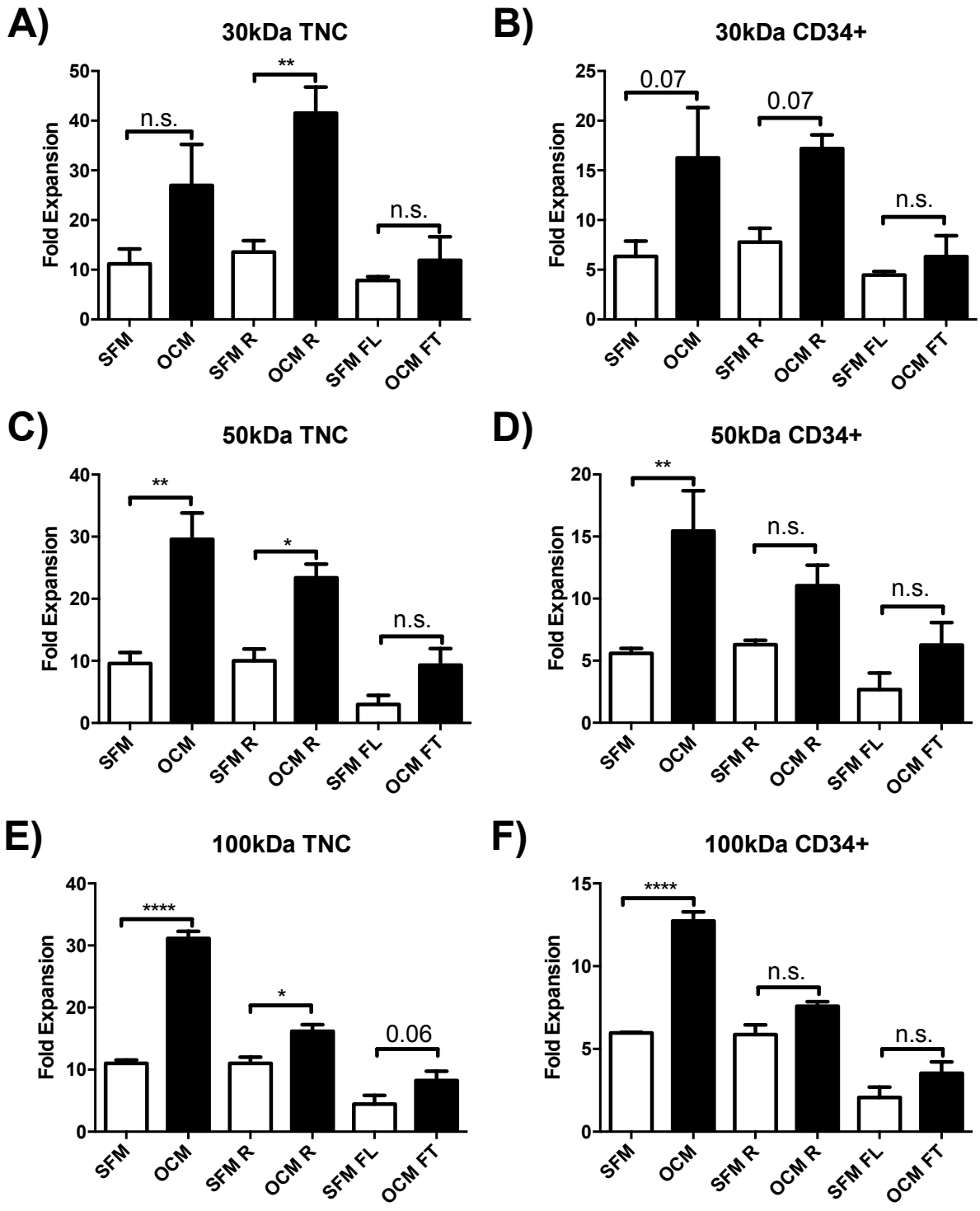

Figure 2: Impact of FASP column fractionation on growth promoting activities of osteoblast conditioned media on CD34+ cells. Production of total nucleated cells or CD34+ from either retentate (R) or flow through (FT) generated by either 30kDa (A-B), 50kDa (C-D) or 100kDa (E-F) FASP spin columns. Mean ± SEM, n=3, ANOVA; * $p<0.05$, ** $p<0.01$

3.2 Effect of the supplement from the serum-free media on the conditioning process

The removal of the abundant bovine serum albumin from the conditioned media was attempted next, to test whether bovine serum albumin was required for secretion of growth modulating targets from the osteoblast conditioned media. The osteoblast conditioned media was produced with either complete serum-free media, or serum-free media without BIT (bovine serum albumin, insulin and transferrin) or first stimulated with complete serum-free media and then replaced with serum-free media without BIT for the last 12 hours. This last condition we will refer to as CHASE moving forward. The concentration of all BIT elements was re-adjusted accordingly for all UCB cultures set up with the different media to allow for a fair comparison of the different media. Again, serum-free media compared to osteoblast condition media showed a significant increase in both total nucleated cell and CD34+ cell expansion ($p=0.011$; $p=0.0006$, respectively) (Figure 3A, 2B). When the supplement BIT was removed from the conditioning process, the growth modulating activity of the osteoblast conditioned media was lost. This result indicates that the secretion of the growth modulating activity requires the BIT supplement. The CHASE osteoblast conditioned media did not see the same magnitude of expansion compared to the complete osteoblast conditioned media; it nonetheless increased the expansion of both total nucleated cells and CD34+ cells over control ($p=0.04$; $p=0.03$, respectively).

An attempt at adding only the bovine serum albumin, insulin and transferrin individually during the conditioning process was attempted but replicating the growth modulating effects of the proprietary blend of BIT from StemCell Technologies could not be achieved and thus was abandoned after several unsuccessful trials. These results

indicate that the BIT supplement is required for the secretion of the growth modulating activity and/or to maximize their activity. The CHASE method provided a viable method for producing conditioned media from osteoblasts that can be used to identify secreted targets, while reducing the background and still being relevant to previously published literature by the Pineault laboratory.

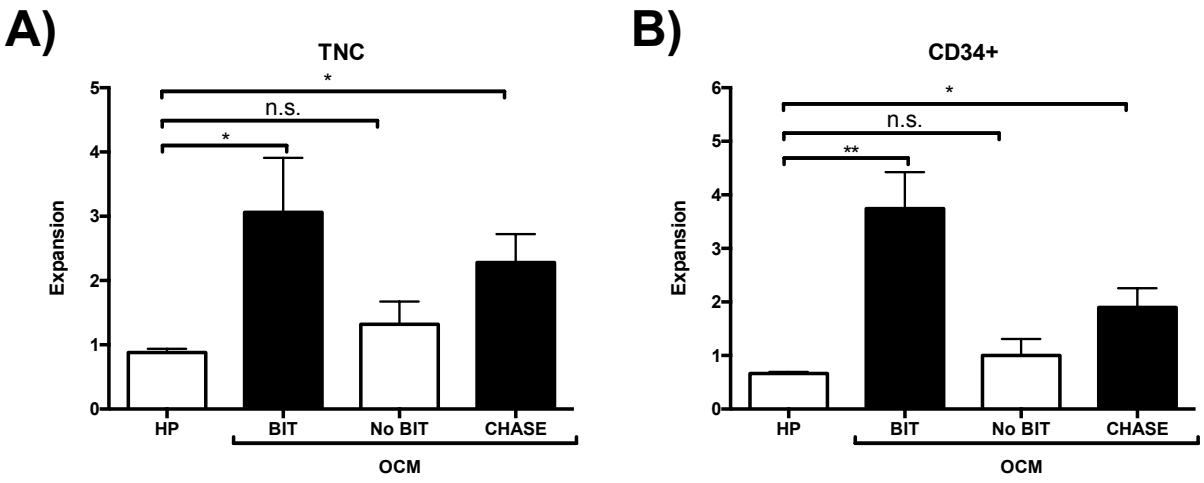

Figure 3: Comparison of osteoblast conditioning methods on HSPC expansion. Expansion of (A) total nucleated cells and (B) CD34+ with either osteoblast conditioned media produced with either BSA, Insulin and Transferrin (BIT) cocktail, absence of BIT cocktail or after 12-hour stimulation with cocktail followed by absence of the cocktail. All components were equalized after conditioning prior to culture of the CD34+ cells. Mean±SEM, n=3, ANOVA; * $p<0.05$

3.3 Comparison of secreted proteins from mesenchymal stem cell and osteoblast conditioned media with mass spectrometry

To produce osteoblast conditioning media for the analysis of the secretome the CHASE method was selected. A comparison between conditioned media from HSPCs and immature osteoblasts (day 6) was performed using MS. To identify factors that promote increased total nucleated cells. Shared factors between the two conditions will give insight into shared properties such as promotions of colony forming cells-G/M/GM and CD34+CXCR4+LFA-1+ population. Post-harvesting of the conditioned media, cells were examined for changes in cell death using Annexin V/Sytox viability assay. HSPCs and osteoblast samples showed no differences in viability (Figure 4E).

The conditioned media was prepared from four independent bone marrow donors and were analyzed by LC-MS/MS which identified a total of 702 proteins from all samples. An assessment of the quality of the data was completed by checking distribution, correlation and principal component analysis. Filtering of targets with valid values in 3 out of the 4 replicates reduced identified proteins to 319. The distribution of each sample was assessed using histograms to check for normal distributions (Figure 4C). The correlation between all samples were compared between all MSC conditioned media samples showing a Pearson's correlation of greater than 0.783 (Figure 4A). The correlation between all osteoblast conditioned media samples had a Pearson's correlation greater than 0.788 (Figure 4B). Using a type of unsupervised learning, known as principal component analysis, comparing both the HSPC conditioned media and osteoblast conditioned media samples and showed a significant separation in component 1 between the two types of cells ($p=0.0055$) (Figure 4D). There were no

observed changes between HSPC conditioned media and osteoblast conditioned media in component 2-7. Both the HSPCs and osteoblasts cluster among themselves within the first dimension showing that they have a similar secretome profile among themselves within the first dimension of variation in the data.

From the filtered targets, 39 were upregulated in osteoblast conditioned media, while eight were down-regulated (Table 3). The “test statistic” assigns a score to each protein based on the difference in expression and the standard deviation. Using a permutation-based method the “test statistic” sets a threshold to identify the chance of a false discovery rate. Higher test statistic scores correlate with lower false discovery rates. Comparing the intensity with the test statistic, four proteins with a high “test statistic” and intensity, cluster away from the rest which include IGF2, cartilage oligomeric matrix protein (COMP), CFD and COL11A1 (Figure 5A).

The UniProt database was used to compare the site of expression data to the upregulated proteins, showing that there was a significant enrichment of known osteoblast genes (47.62-fold, $q= 1.54x10^{-6}$) (Figure 6). This enrichment provides further confidence in our dataset, confirming the origin of the secreted proteins. Next, enrichment for cellular components was evaluated to determine the secretion of proteins. All proteins were enriched to be part of either extracellular space, extracellular region, extracellular matrix, exosome or microvesicle (Figure 7).

The enrichment for biological processes was evaluated to determine potential pathways involved in the growth modulation of HSPCs. From the upregulated proteins 10.8% of proteins were annotated to be involved in ossification, with a fold enrichment of 24 (Figure 8). These included CLEC3B; COL11A1; FSTL3; IGF2; OMD. Also,

proteins involved in the organization of the extracellular matrix, a function of osteoblast cells highly enriched in the upregulated proteins with a 14-fold enrichment. The pathways with the greatest fold enrichment were complement activation (alternative pathway), platelet degranulation and complement activation with 104, 25 and 25-fold enrichment respectively (Figure 8). Based on these gene enrichments, further investigation of the complement pathway and likely more specifically the alternative pathway in the regulation of HSCs, should be investigated.

The proteins significantly upregulated in our study were compared to two previous studies looking at the secretome during osteoblast differentiation at a similar time point, having an overlap of ten-percent with each study (Figure 9B&C). The studies of Kim et al, 2012 and Kristensen et al, 2012 overlapped with the following proteins respectively IGFBP2, IGFBP4, COMP and CFH, and LGALS3 and PLEC. The difference between our study and the studies of Kim et al, 2012 and Kristensen et al, 2012 can be accounted for in the methods that were used to produce the conditioned media. Our study used unfiltered media and a CHASE method while theirs used conditioned media prepared with DMEM and filtered (0.22μm). Previous studies by the Pineault laboratory showed that 0.22μm filtration of osteoblast conditioned media reduces the efficacy which may be removing potential targets [45]. Also, our three studies varied in the type of mass spectrometer used and all of these changes likely contributed to the differences. Additionally, our study and Kim et al., 2012 used independent human HSPC donors with label-free quantification. Kristensen et al., 2012 used a single immortalized hTERT human HSPC line allowing the use of SILAC, which is a more quantitative method. Compared to Kim et al., 2012 and Kristensen et al., 2012 our study showed an

increased enrichment of biological pathways based on the FunRich database for regulation of insulin-like growth factor activity, integrin cell surface interactors and complement pathway (Figure 9A). Therefore, the differences between our studies may guide the selection of candidates with growth modulating effects on HSPCs.

Using label-free quantification, I was able to identify 47 targets potentially involved in the growth modulatory effect on HSPCs, including potentially novel targets. Further screening using gene ontology enrichment and comparisons with other studies has allowed further insights for targeted screening in the future.

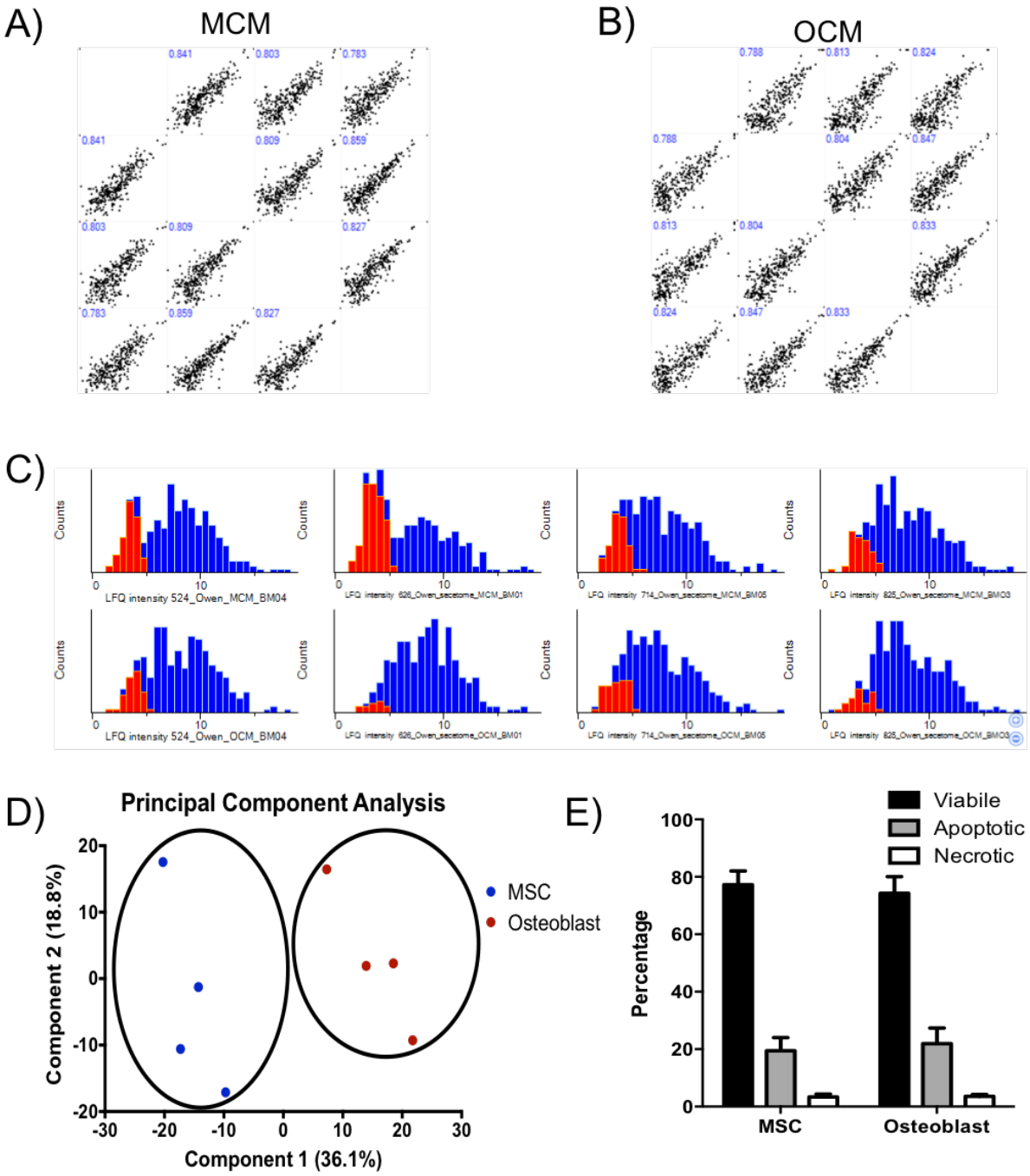

Figure 4: Quality assessment of mass spectrometry data.
Correlations between media conditioned from MSC (A) and osteoblast (B) compared against each other. (C) The distribution of each sample was assessed using 30 bins. The blue bars represent the measured values while the red bars represent imputation values. (D) The variation of the secreted proteins from MSC and osteoblasts are only separated by the first component. (E) Viability of MSC and osteoblast that had their conditioned media harvested.

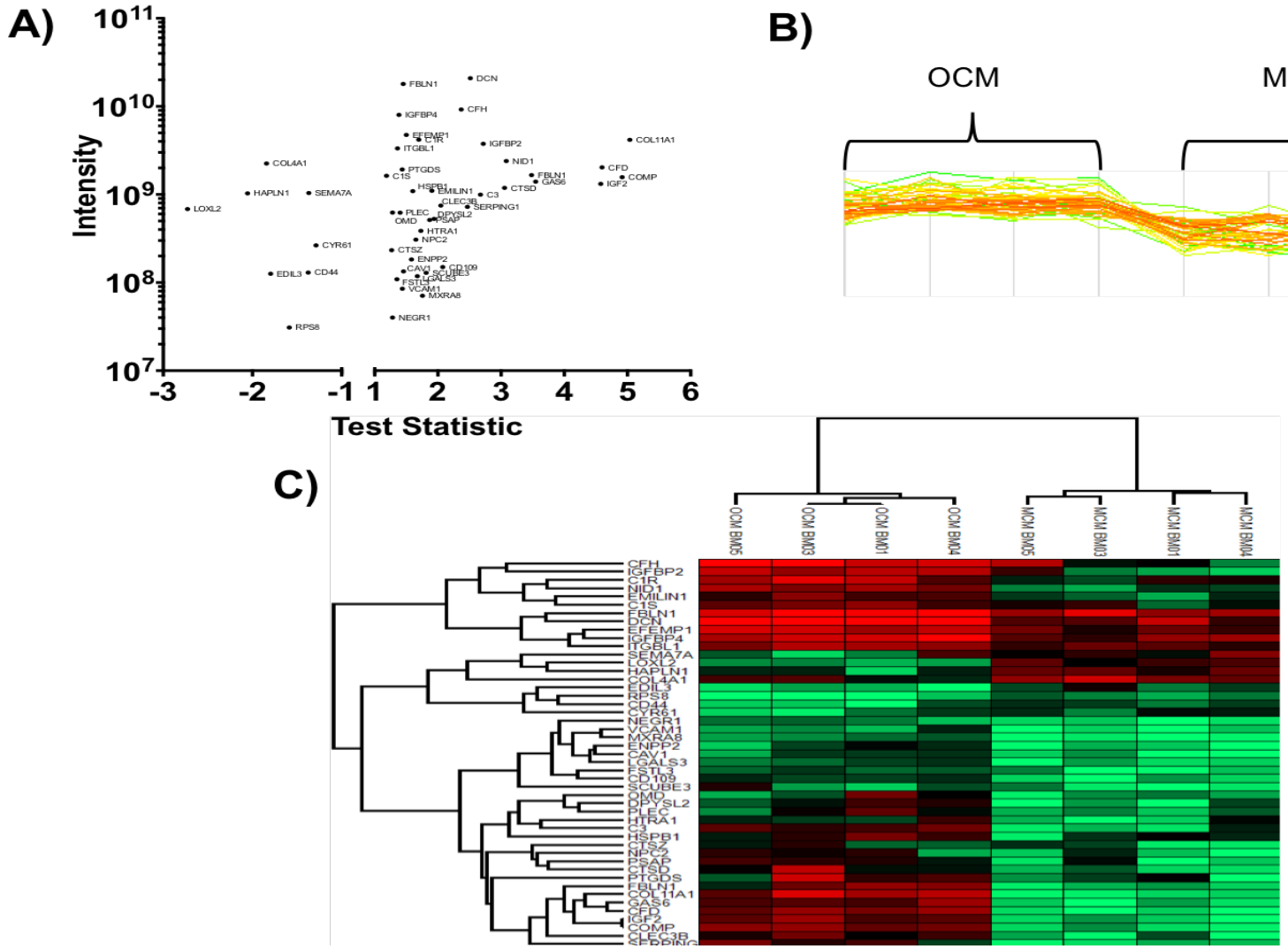

Figure 5: Differentially secreted proteins between MSC and osteoblasts.
(A) Comparing the intensity and student t-test test statistic of differentially regulated proteins. (B) The upregulated regulated proteins in osteoblast conditioned media shown in a line plot compared across donors. (C) Significantly differentially regulated proteins shown in a heatmap clustered using Euclidean distance. n=4

Table 3: Quantification of osteoblast conditioned media against MSC conditioned media using mass spectrometry. Conditioned media generated using the CHASE method and compared using label-free quantification. Mean, n=4, Student T-test; S0=1; targets with q<0.05 with FDR calculated using permutation method set to 250.

Protein names	Gene names	q-value (Permutation)	Test Statistic
Lysyl oxidase homolog 2	LOXL2	0	-2.72767197
Hyaluronan and proteoglycan link protein 1	HAPLN1	0	-2.055059252
Collagen alpha-1(IV) chain;Arresten	COL4A1	0.015047619	-1.841330105
EGF-like repeat and discoidin I-like domain-containing protein 3	EDIL3	0.01373913	-1.795450658
40S ribosomal protein S8	RPS8	0.033333333	-1.586645045
CD44 antigen	CD44	0.035789474	-1.374470253
Semaphorin-7A	SEMA7A	0.034871795	-1.368271262
Protein CYR61	CYR61	0.04847619	-1.287999907
Complement C1s subcomponent	C1S	0.036555556	1.186993991
Cathepsin Z	CTSZ	0.045244444	1.268842318
Neuronal growth regulator 1	NEGR1	0.046272727	1.2819161
Plectin	PLEC	0.047348837	1.282353762
Follistatin-related protein 3	FSTL3	0.033170732	1.351324111
Integrin beta-like protein 1	ITGBL1	0.034	1.361476148
Insulin-like growth factor-binding protein 4	IGFBP4	0.036756757	1.384495339
Osteomodulin	OMD	0.024142857	1.402989682
Prostaglandin-H2 D-isomerase	PTGDS	0.027777778	1.435042346
Vascular cell adhesion protein 1	VCAM1	0.028571429	1.437193592
Fibulin-1	FBLN1	0.029411765	1.451091661
Caveolin-1	CAV1	0.03030303	1.457646837
EGF-containing fibulin-like extracellular matrix protein 1	EFEMP1	0.03125	1.501142241
Ectonucleotide pyrophosphatase/phosphodiesterase family member 2	ENPP2	0.032258065	1.581259922
Heat shock protein beta-1	HSPB1	0.034482759	1.601983766
Epididymal secretory protein E1	NPC2	0.035714286	1.652423344
Galectin-3	LGALS3	0.023703704	1.673887355
Complement C1r subcomponent	C1R	0.024615385	1.69834786
Serine protease HTRA1	HTRA1	0.0256	1.731753577
Matrix-remodeling-associated protein 8	MXRA8	0.026666667	1.756444469
EGF-like domain-containing protein 3	SCUBE3	0.014363636	1.814200806
Prosaposin	PSAP	0.0158	1.870018822
EMILIN-1	EMILIN1	0.016631579	1.90561131
Dihydropyrimidinase-related protein 2	DPYSL2	0	1.938934489

Tetranectin	CLEC3B	0	2.046031137
CD109 antigen	CD109	0	2.076810592
Complement factor H	CFH	0	2.370114951
Plasma protease C1 inhibitor	SERPING1	0	2.466247771
Decorin	DCN	0	2.514067025
Complement C3	C3	0	2.674998728
Insulin-like growth factor-binding protein 2	IGFBP2	0	2.717205462
Cathepsin D	CTSD	0	3.055543189
Nidogen-1	NID1	0	3.083136072
Fibulin-1	FBLN1	0	3.483066622
Growth arrest-specific protein 6	GAS6	0	3.548397791
Insulin-like growth factor II	IGF2	0	4.577966013
Complement factor D	CFD	0	4.597355563
Cartilage oligomeric matrix protein	COMP	0	4.916610636
Collagen alpha-1(XI) chain	COL11A1	0	5.037889708

A)

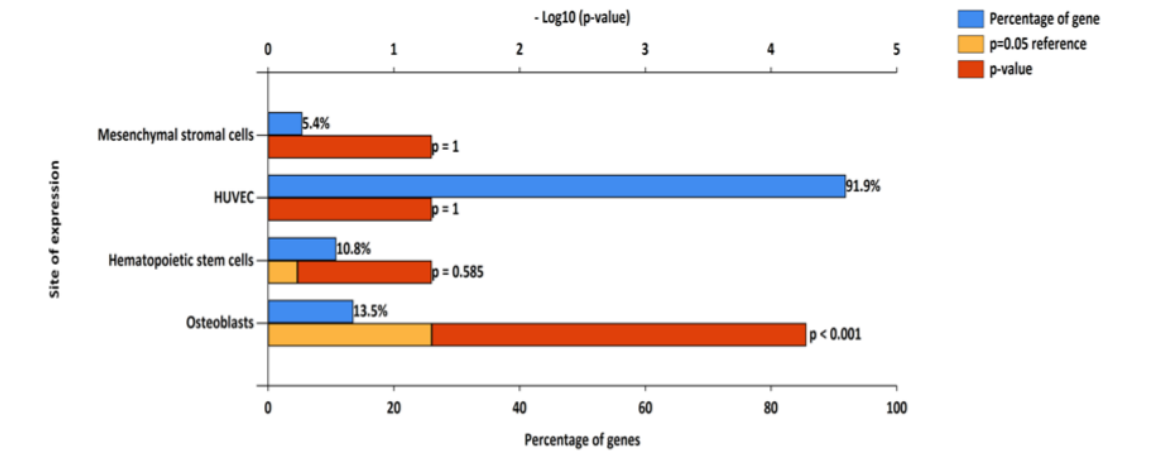

B)

Site of expression	No. of genes in the dataset	No. of genes in the background dataset	Fold enrichment	q-value	Genes mapped
Osteoblasts	5	52	47.62	1.544E-06	ITGBL1; IGFBP4; FBLN1; SCUBE3; CLEC3B;
Mesenchymal stromal cells	2	178	5.58	0.17808	CAV1; CD109;

Figure 6: Enrichment of the origin of proteins secreted by MSC-derived osteoblasts. Enrichment for tissue of origin from proteins upregulated in osteoblast secretome. The background datasets taken from FunRich on March 14, 2018.

A)

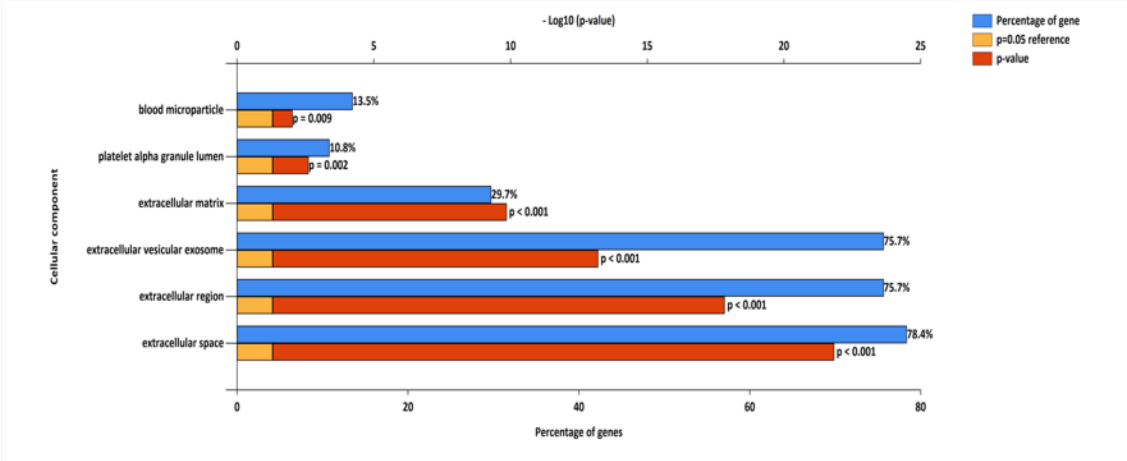

B)

Cellular component	No. of proteins in the dataset	No. of proteins in the background dataset	Fold enrichment	q-value	proteins mapped
extracellular space	27	1385	9.65	1.134E-19	C1R; C3; CD109; CFH; CLEC3B; COL11A1; COMP; CTSD; CTSZ; DCN; EFEMP1; EMILIN1; ENPP2; FBLN1; FSTL3; GAS6; HSPB1; HTRA1; IGFBP2; IGFBP4; ITGBL1; LGALS3; PSAP; PTGDS; SCUBE3; SERPING1; VCAM1
extracellular region	28	1842	7.52	4.018E-18	C1R; C1S; C3; CD109; CFD; CFH; CLEC3B; COL11A1; COMP; CTSD; CTSZ; DCN; EFEMP1; EMILIN1; FBLN1; FSTL3; GAS6; HTRA1; IGF2; IGFBP2; IGFBP4; LGALS3; NEGR1; NID1; NPC2; PSAP; PTGDS; SERPING1
extracellular exosome	28	2772	5.00	1.622E-13	C1R; C1S; C3; CFD; CFH; CLEC3B; COMP; CTSD; CTSZ; DPYSL2; EFEMP1; EMILIN1; FBLN1; GAS6; HSPB1; HTRA1; IGF2; IGFBP2; LGALS3; MXRA8; NEGR1; NID1; NPC2; PLEC; PSAP; PTGDS; SERPING1; VCAM1
extracellular matrix	8	268	14.78	2.057E-05	DCN; EMILIN1; HSPB1; HTRA1; LGALS3; NID1; OMD; PLEC; PSAP
blood microparticle	5	175	14.16	5.935E-03	C1R; C1S; C3; CFH; SERPING1

Figure 7: Enrichment of secreted proteins in different cellular components. Enrichment of cellular components from proteins upregulated in osteoblast conditioned media. The background datasets taken from FunRich on March 14, 2018.

A)

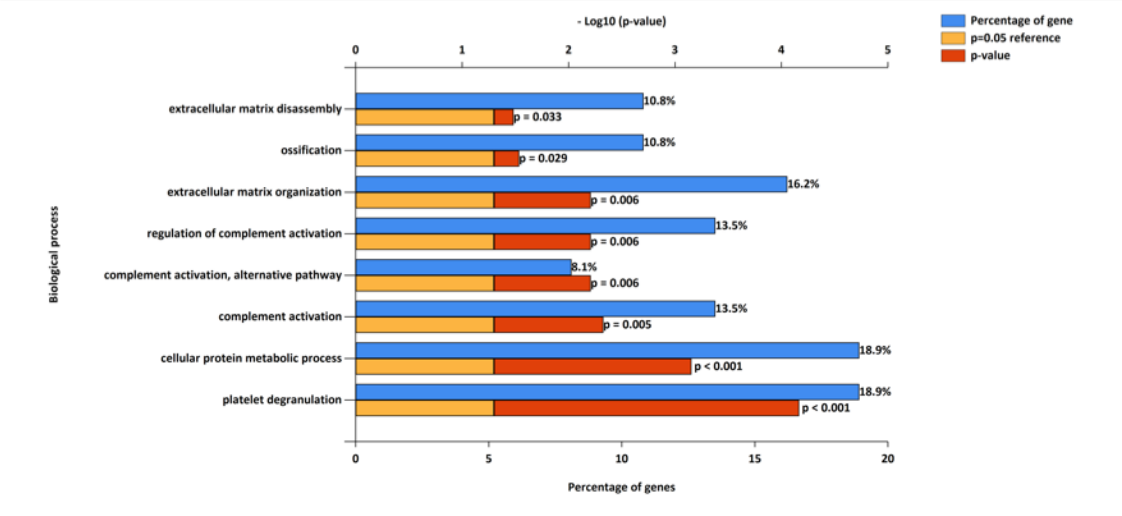

B)

Biological Processes	No. of proteins in the dataset	No. of proteins in the background dataset	Fold enrichment	q-value	proteins mapped
platelet degranulation	7	124	25.47	1.06E-04	CD109; CFD; CLEC3B; GAS6; IGF2; PSAP; SERPING1
cellular protein metabolic process	7	192	16.45	1.09E-03	C3; FSTL3; GAS6; IGF2; IGFBP2; IGFBP4; MXRA8
complement activation	5	91	24.80	6.44E-03	C1R; C1S; C3; CFD; CFH
complement activation, alternative pathway	3	13	104.23	8.31E-03	C3; CFD; CFH
regulation of complement activation	5	108	20.90	8.95E-03	C1R; C1S; C3; CFH; SERPING1
extracellular matrix organization	6	199	13.60	8.95E-03	COL11A1; COMP; DCN; FBLN1; NID1; VCAM1
ossification	5	75	24.08	3.63E-02	CLEC3B; COL11A1; FSTL3; IGF2; OMD
extracellular matrix disassembly	4	77	23.46	3.63E-02	DCN; HTRA1; NID1; SCUBE3

Figure 8: Enrichment of secreted proteins involved in different biological processes. Enrichment of biological processes from proteins upregulated in osteoblast conditioned media. The background datasets taken from FunRich on March 14, 2018.

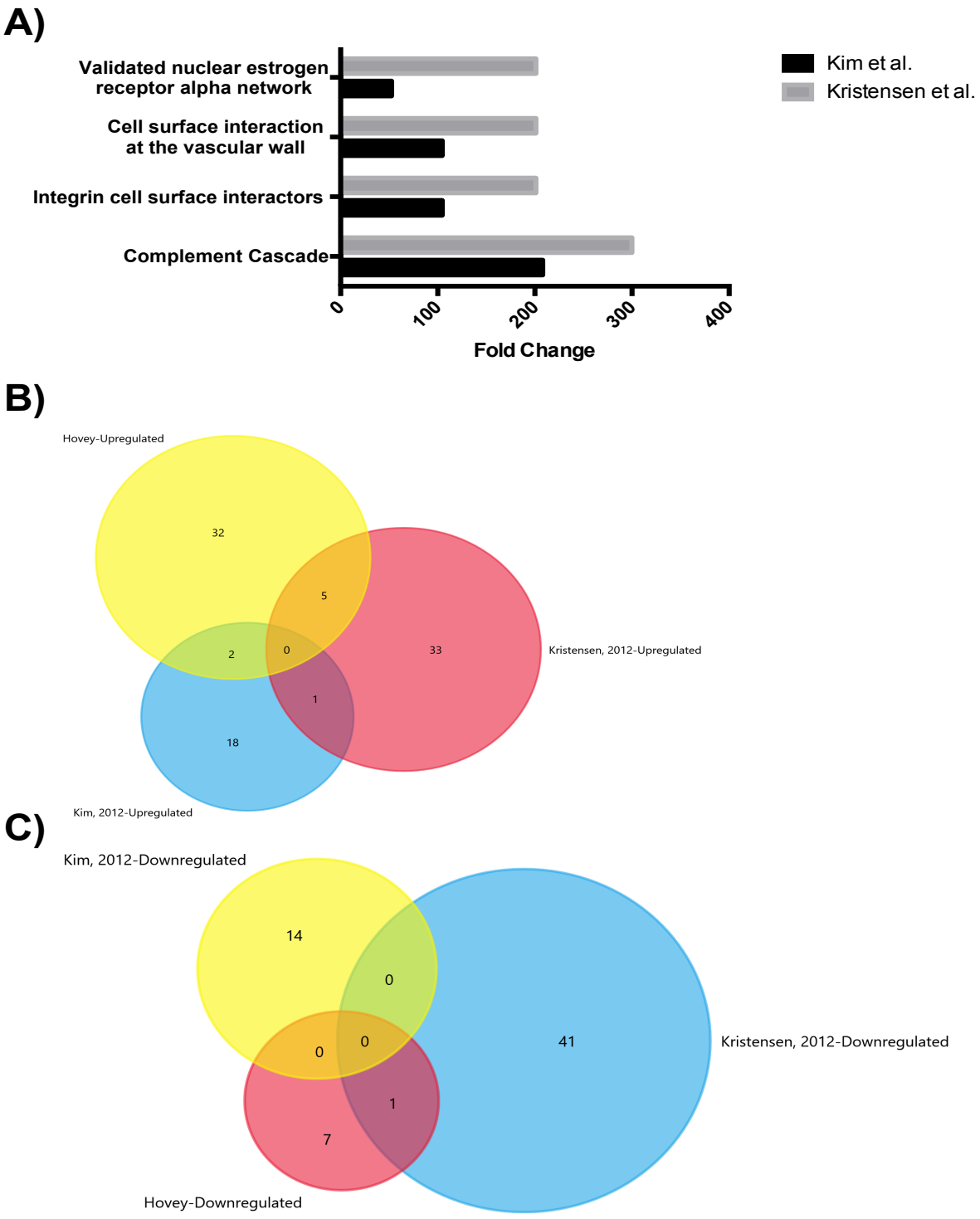

Figure 9: Comparison to previous early osteoblast differentiation studies. (A) Comparing the differences in fold enrichment between proteins upregulated during osteogenic differentiation from our study and Kim et al, 2012 & Kristensen et al, 2012. Venn diagrams comparing the overlap and differences of the (B) upregulated and (C) downregulated proteins between our dataset and the datasets from Kim et al, 2012 & Kristensen et al, 2012

3.4 Validation of differentially expressed proteins through gene expression

Testing of the gene expression of 11 differentially regulated secreted proteins was done to confirm the validity of the MS results. Reference genes were compared for stability using GeNorm, and then RPL13a, RPLP0, TBP and HPRT1 were selected as stable and had an M-value of less than 0.5. GAPDH was significantly upregulated during differentiation and therefore excluded as a reference gene. From the ten selected secreted proteins observed to be upregulated in the MS results, all of them showed an increase in their transcript gene expression in osteoblasts, relative to the undifferentiated HSPCs (Figure 10). Moreover, I confirmed that one of the proteins observed to be decreased by MS during osteogenic differentiation was also lower at gene expression level (LOXL12: 4.6-fold decrease, p=0.015). The pathway with the greatest fold enrichment was the complement pathway, and therefore I focused on the validation of several corresponding genes. The five complement factors all had their gene expression upregulated in osteoblasts, and this included C3, CFD, CFH, C1S and C1R.

Previous results in the Pineault lab had shown that osteoblast conditioned media decreased apoptosis of HSPCs in cytokine starved cultures (Abu-Khader, Manuscript Submitted). A possible expansion of this is an extracellular matrix protein involved in inhibiting apoptosis known as COMP, which was also validated (qPCR: 34.7-fold, p=0.029; MS: 87.4-fold, p=0.00024) (Figure 10)[81,82]. Another possible explanation for the decrease in apoptosis is CD109, which I also validated (qPCR: 3.9-fold, p=0.004), a protein known to block TGFβ signalling [83].

Both GAS6 and decorin were previously implicated in the support of HSPCs and therefore selected for further evaluation. GAS6 targets multiple phosphotyrosine receptors including Axl, Sky and Mer. GAS6 maintains progenitors (colony forming cells), but the mechanism of action for this is still unknown. [84]. GAS6 is also involved in natural killer cell development during IL-15 mediated differentiation through the Axl receptor [85]. This study also showed that primary CD34+ cells only express Axl and Mer receptors. Decorin is an extracellular matrix protein that has been shown to have a similar effect to the addition of Wnt3a to HSPCs leading to maintenance of HSCs. Both GAS6 and decorin were found upregulated in osteoblasts when compared to MSC (Figure 10).

Previous studies by the Pineault laboratory also showed confirmation of MS results. Dumont et al. reported an increase in IGFBP2 secretion using an antibody array in osteoblasts over HSPCs [45]. Kyle Law showed that osteoblasts secrete more significant levels of IGF2 that HSPCs using an enzyme-linked immunosorbent assay (Abu-Khader et al., Manuscript Submitted). Our gene expression data coupled with those studies provide high confidence in the validity of the MS results.

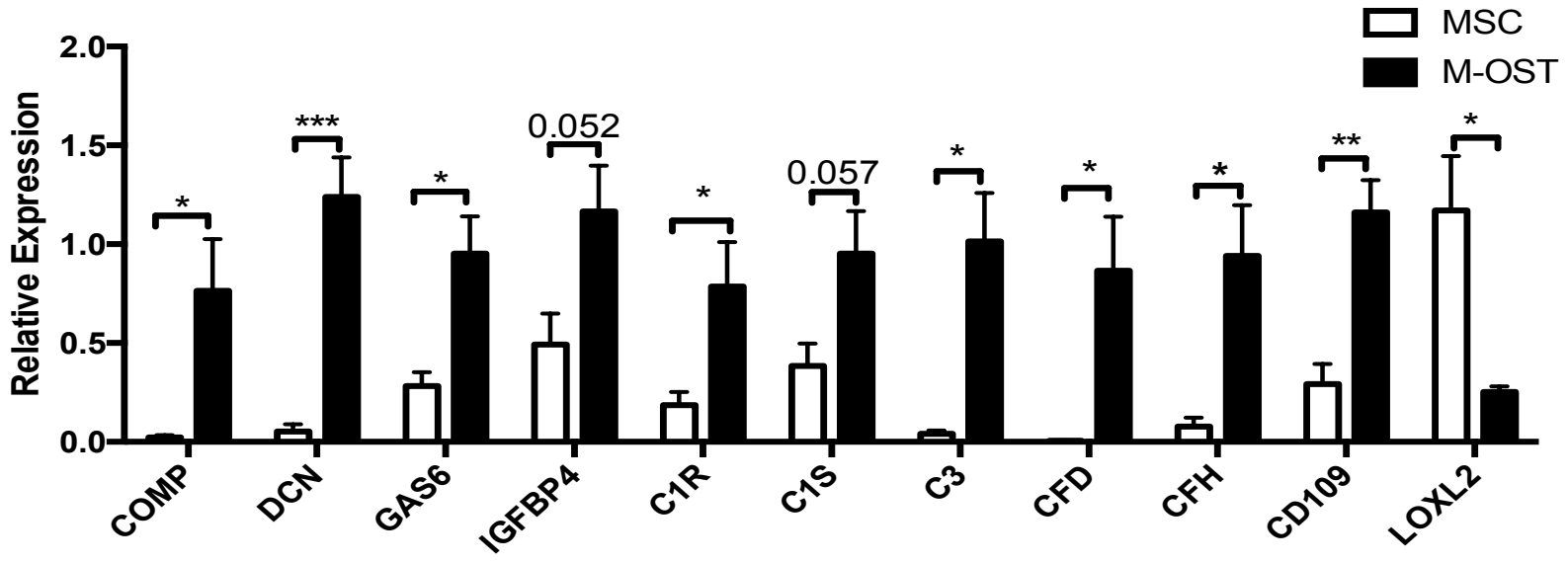

Figure 10: Validation of up-regulated osteoblast secretome candidates using gene expression. Comparison of HSPC gene expression in day 6 immature osteoblasts and parental MSC. Mean±SEM, n=4, Student T-test; * $p<0.05$, ** $p<0.01$, *** $p<0.001$

3.5 Effect of galectin-3 on the production of MMP in *ex vivo* culture

One protein identified in our screening as upregulated in osteoblast conditioned media is galectin-3, which is part of the lectin family of proteins with a diverse set of roles dependent on if galectin-3 is found intracellularly or extracellularly [86]. Extracellularly, these diverse set of roles include induction of apoptosis and migration of cells and neutrophil and mast cell activation. While intracellularly galectin-3 has been shown to inhibition apoptosis and promote β-catenin activation through multiple mechanisms [87,88]. Additionally, the effect of galectin-3 seems to be cell type specific and responses can vary widely [86]. I set out to test whether galectin-3 could mimic some of the proliferative activity of osteoblast conditioned media on CB CD34+ cells. Concentrations between 1ng/mL to 100ng/mL was screened during the first replicate and I choose to focus on 10ng/ml and 20ng/ml for the following replicates. The addition of galectin-3 at 10ng/mL lead to a significant decrease in the expansion of CD34+CD45RA-CD38-CD90- (MPP) population (1.7-fold, p=0.04) (Figure 9). The addition of 20ng/mL of galectin-3 decreased the expansion of the MMP population, though it was not significant. Similar results were observed for the production of CD34+CD45RA-CD38-CD90+ HSC-enriched cells though differences were not significant. At either dose tested, galectin-3 had no significant impact on the expansion of total nucleated cells or CD34+ cells. The use of recombinant galectin-3 on hematopoietic progenitor and stem cells has been shown here to have a negative effect on their expansion.

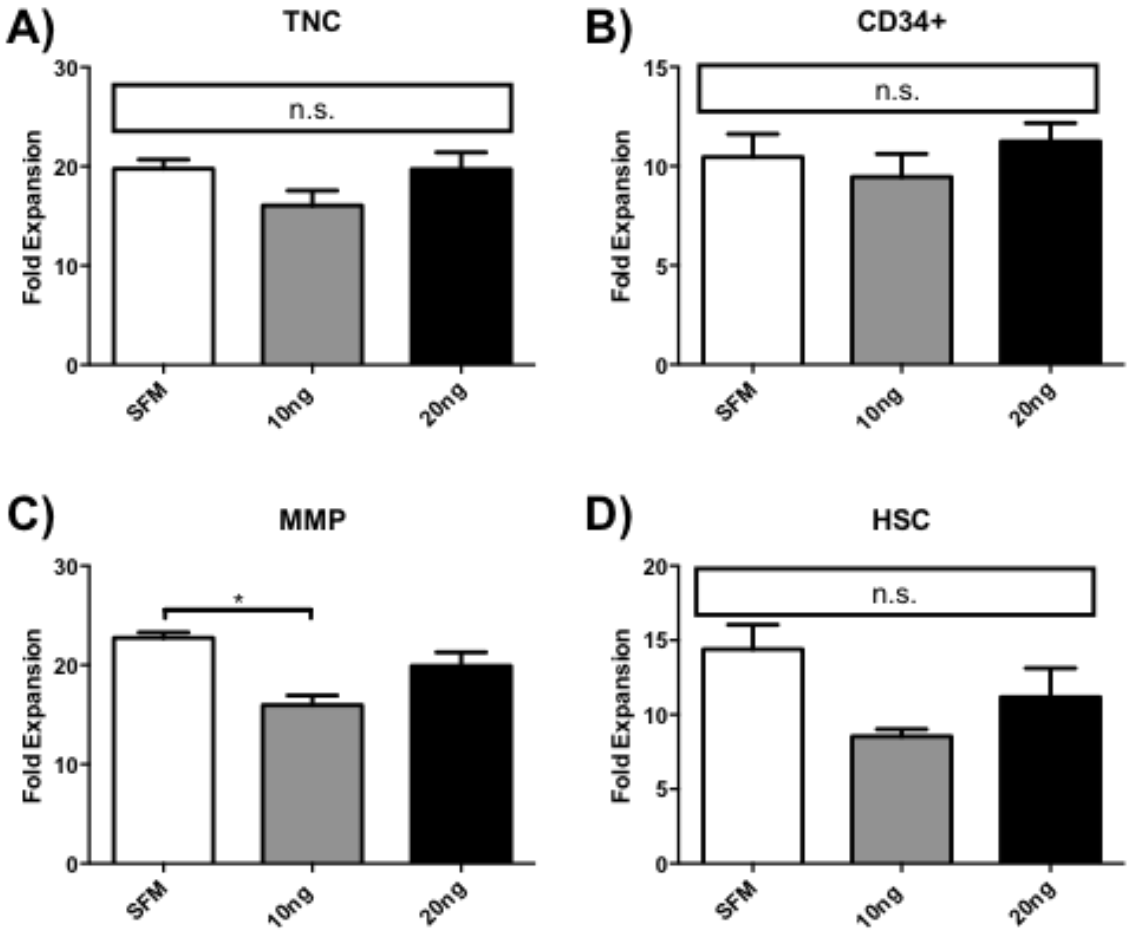

Figure 11: Addition of recombinant galectin-3 to HSPC culture. Expansion of total nucleated cells (A), CD34+cells (B), CD34+CD45RA- cells (C) and MMP (D) after 6 days in culture. Mean ± SEM, n=3, ANOVA; * $p<0.05$

3.6 Soluble SPARC leads to expansion of HSPC populations

Previous work using decellularized osteoblasts showed that extracellular matrix from osteoblasts promoted *ex vivo* expansion of HSCs [62]. Examining high abundant matrix proteins from the MS results, I choose to study the potential contribution of SPARC. The role and importance of SPARC in hematopoiesis are controversial at present. Knockouts in zebrafish have been associated with hematopoietic deficiencies [89]. In conflicting studies using SPARC deficient murine models, one showed no significant hematopoietic deficiencies and performed just as well as the wild-type in a competitive transplant [90], while the other SPARC deficient murine model shows deficiencies in platelet counts and BFU-E colony forming cells [91]. Murine HSCs do not express SPARC, unlike human HSCs, suggesting SPARC may have a different role in different species [90]. SPARC is one of the highest expressed proteins when HSC colonize the bone marrow from the liver [92]. Concentrations between 1ng/mL to 100ng/mL was screened during the first replicate and I choose to focus on 10ng/ml and 20ng/ml for the following replicates. The addition of low quantities of SPARC had no significant effects on the number of total nucleated cells and CD34+ cells in culture. However, the addition of 10ng of SPARC moderately promoted the production of multiple populations enriched in stem and progenitors including, CD34+CD45RA- (1.3-fold increase, p=0.0012) and CD34+CD45RA-CD38-CD90- (MPP) (1.4-fold increase, p=0.0013) population (Figure 12). There were no significant effects observed for the HSC-enriched subpopulation, defined herein as CD34+CD45RA-CD38-CD90+ cells. Here I show that SPARC has a modest effect on the growth of HSPCs.

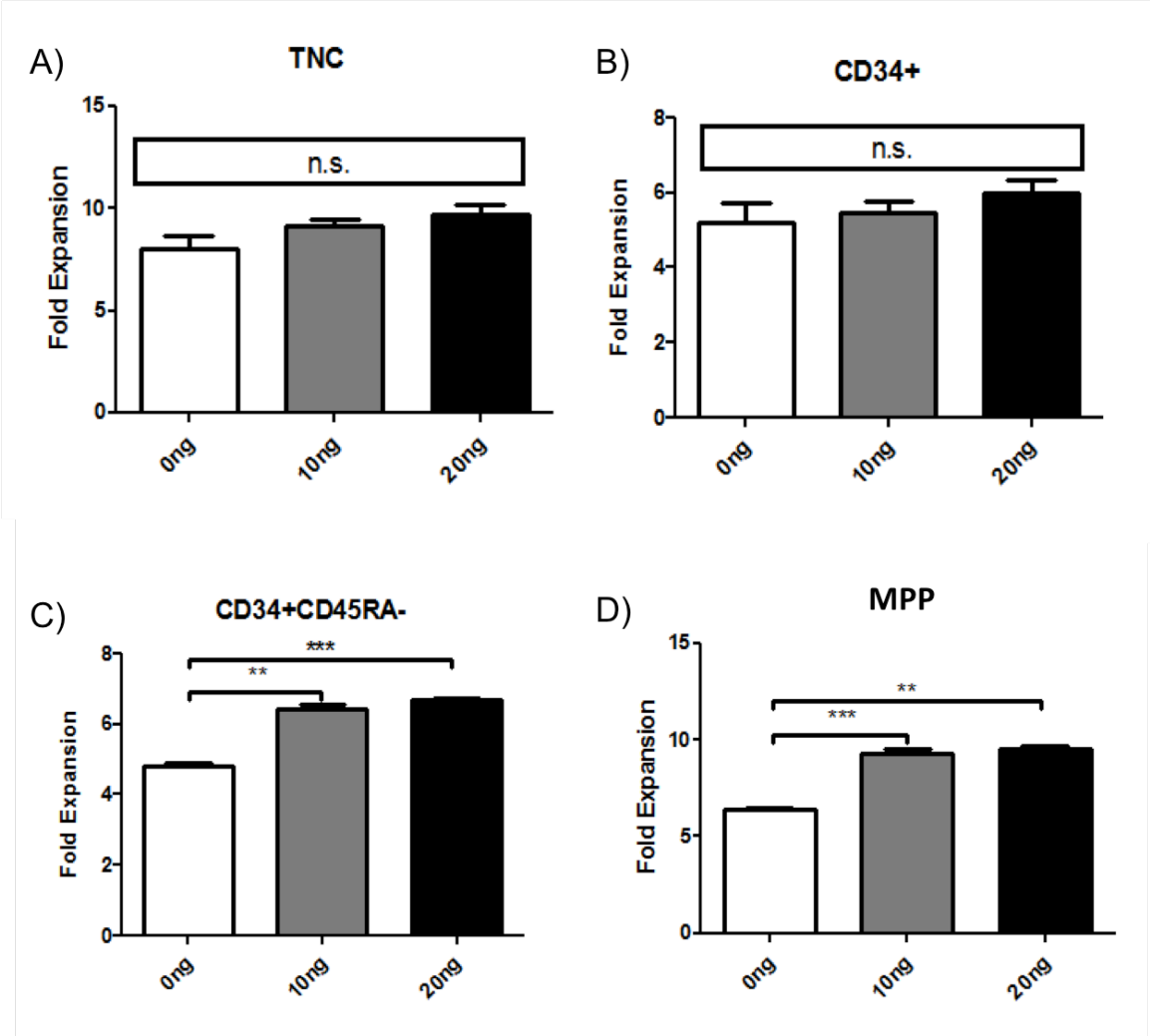

Figure 12: Addition of recombinant SPARC to CD34+ cell culture.
Expansion of total nucleated cells (A), CD34+ (B), CD34+CD45RA- (C), MMP (D) after 6 days in culture. Mean±SEM, n=4, ANOVA; * $p<0.05$.

3.7 Overlap of microvesicles and exosome proteins with osteoblast secreted proteins

Investigating the overlap between our dataset and proteins found in extracellular vesicles is important as there was an enrichment of microparticles and exosomes observed in the upregulated proteins. To examine the potential of microvesicles and exosomes in osteoblast conditioned media, I compared the proteins detected by MS and the Vesiclepedia database (Figure 13). When comparing all proteins detected in osteoblast conditioned media to microvesicles, there was a 68.6% overlap (219/319) and an overlap of microvesicles of 51.3% (20/39) with secreted proteins upregulated from osteoblast. When comparing exosomes 91.2% (291/319) overlapped with all secreted proteins detected from osteoblasts and 86.4% (33/39) overlapped with secreted proteins upregulated from osteoblasts. The lower overlap of osteoblast secreted targets with microvesicles compared to exosomes can be partially attributed to the fact that microvesicles are studied less than exosomes[63]. This comparison suggests the detection of either microvesicles or exosomes in the osteoblast secretome.

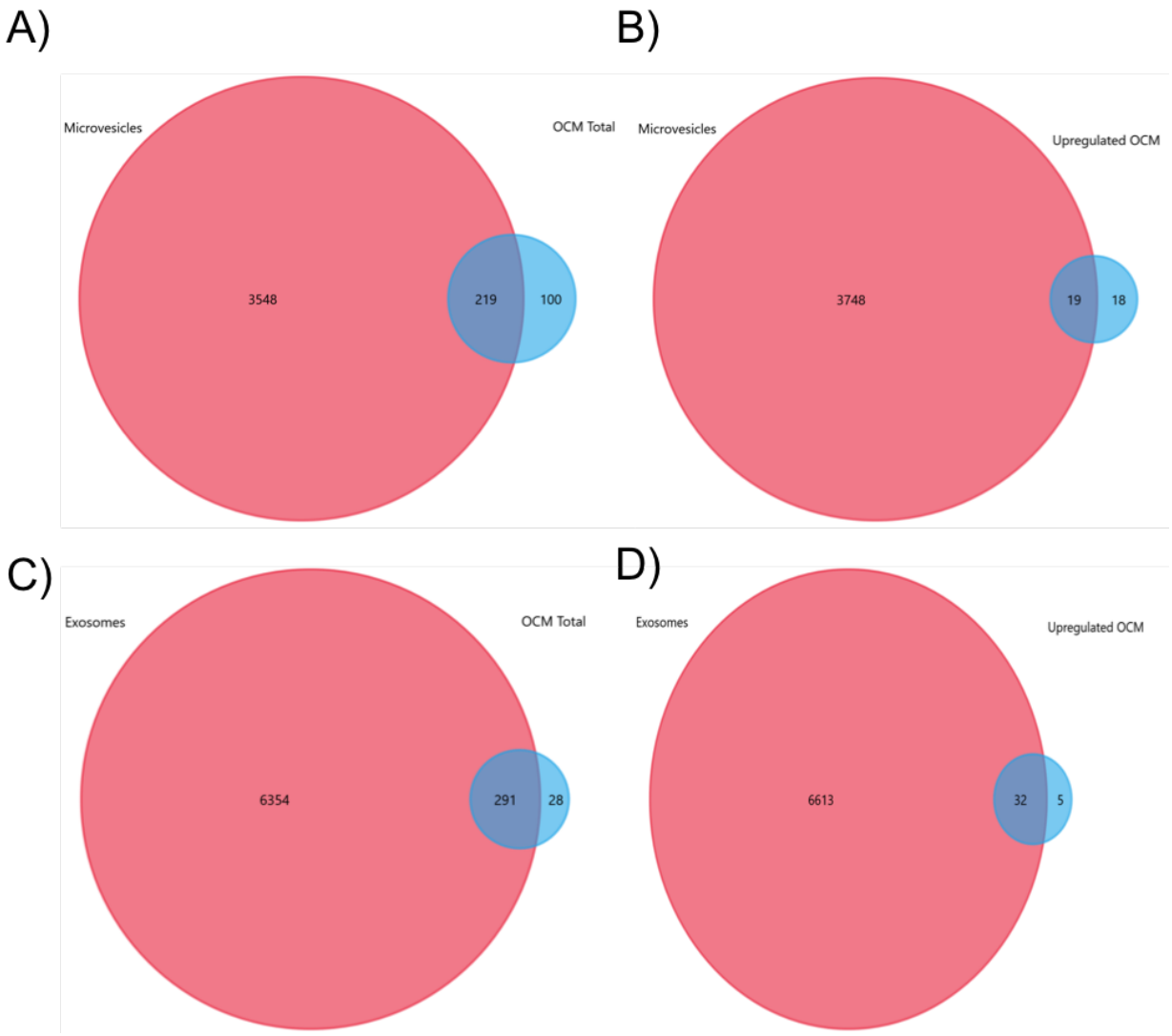

Figure 13: Overlap of osteoblast secreted proteins with microvesicles and exosomes. Microvesicle (A, B) and exosome (C, D) datasets were taken from Vesiclepedia database on March 14, 2018 and compared to all proteins detected (A, C) and up-regulated proteins (B, D).

3.8 Characterization of microvesicles present in osteoblast conditioned media

Based on the overlap of osteoblast secretome with microvesicles and previous work filtering osteoblast conditioning media I decided to isolate and characterize microvesicles in our osteoblast conditioned media. Previous studies showed that osteoblasts can secrete microvesicles [68]. It is important to confirm the characteristics of microvesicles or matrix vesicles secreted by our serum-free conditioned media as changes in the media produce different microvesicle sizes and protein contents [66]. A microvesicle isolation protocol based on centrifugation of 20,000xg for 20 minutes was used to assess their presence in osteoblast conditioned media, and particles were analyzed using the Zetaview for detection and size determination. Due to the similarities between microvesicles and matrix vesicles and that the test to differentiate between them was not done, henceforth I will refer to the microparticles isolated as microvesicle-like particles. Microparticles detected in microvesicle enriched fraction had an average peak size of 132.9nm±8.1 (Figure 14B). Particles with these size profiles match size profiles of microvesicles and matrix vesicles. Size profiles from osteoblast microvesicle-like particles match that from the more extensively studied HSPC microvesicles [93]. Further characterization of the microvesicle-like particles using flow cytometry confirmed the presence of phosphatidylserine using Annexin V staining, a marker for extracellular vesicles (Figure 14A). There was a significant upregulation in the secretion of VCAM-1 (CD106) found in the proteomics osteoblast conditioned media samples, which can be found on the surface of cells and extracellular vesicles and secreted [94,95]. Staining of microvesicle-like particles for CD106 showed 28.7% and 15.7% positive for CD106 in the Annexin V+ particles for two of the donors while the third only showed 4.22%

(Figure 14A). Based on these complementary results, I concluded that there is a high confidence that our conditioning method produces microvesicles or matrix vesicles from immature osteoblasts.

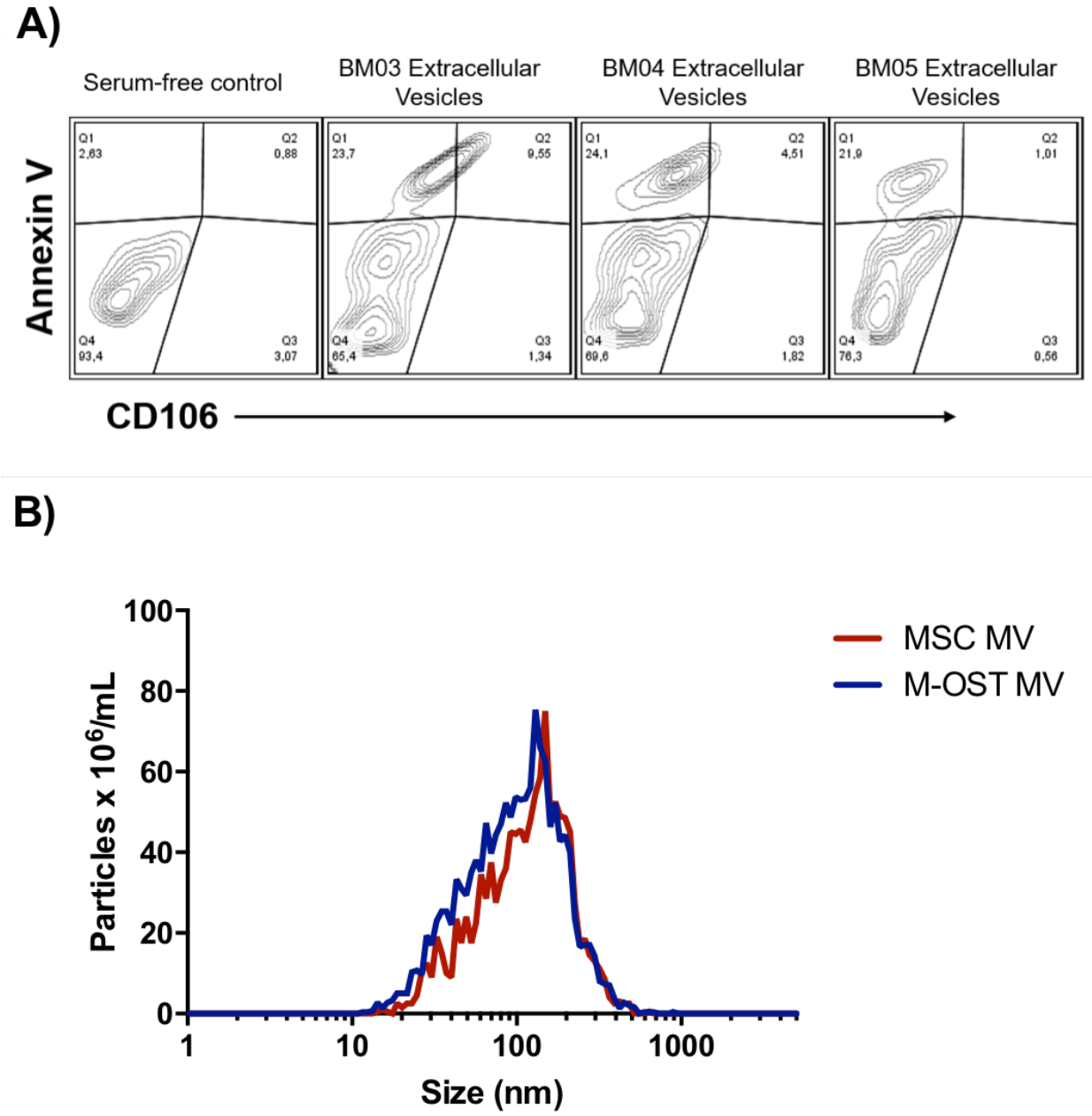

Figure 14: Characterization of microvesicle-like particles from immature osteoblasts.
Extracellular particles from conditioned media concentrated by centrifugation. A) Annexin V and CD106 staining on microvesicles isolated from osteoblasts from three representative samples compared to particles isolated from serum-free media. B) Size comparison of microvesicles from osteoblast and HSPCs. n=2, MSC; n=3, osteoblasts.

3.9 Depletion of microvesicles-like particles from osteoblast conditioned media

Next, I tested if the reduction in microvesicle-like particles in osteoblast conditioned media by centrifugation would change the modulatory growth activities of osteoblast conditioned media on UCB CD34+ cells. Reduction of microvesicle-like particles decreased the expansion of UCB CD34+ cells in osteoblast conditioned media as shown by the significant reduction in total nucleated cells ($p=0.0021$), though the microvesicle-like particles depleted condition, still showed an increase over the serum-free control ($p=0.0076$) (Figure 15A). A reduction in microvesicle-like particles in osteoblast conditioned media reduced the overall production of CD34+ cells and other CD34+ subpopulations to levels midway between osteoblast conditioned media and serum free media controls, though there were no significant differences between osteoblast conditioned media and microvesicle-like particle depleted media. These preliminary results suggest that part of the osteoblast growth modulating effects may be mediated or regulated by microvesicle-like particles.

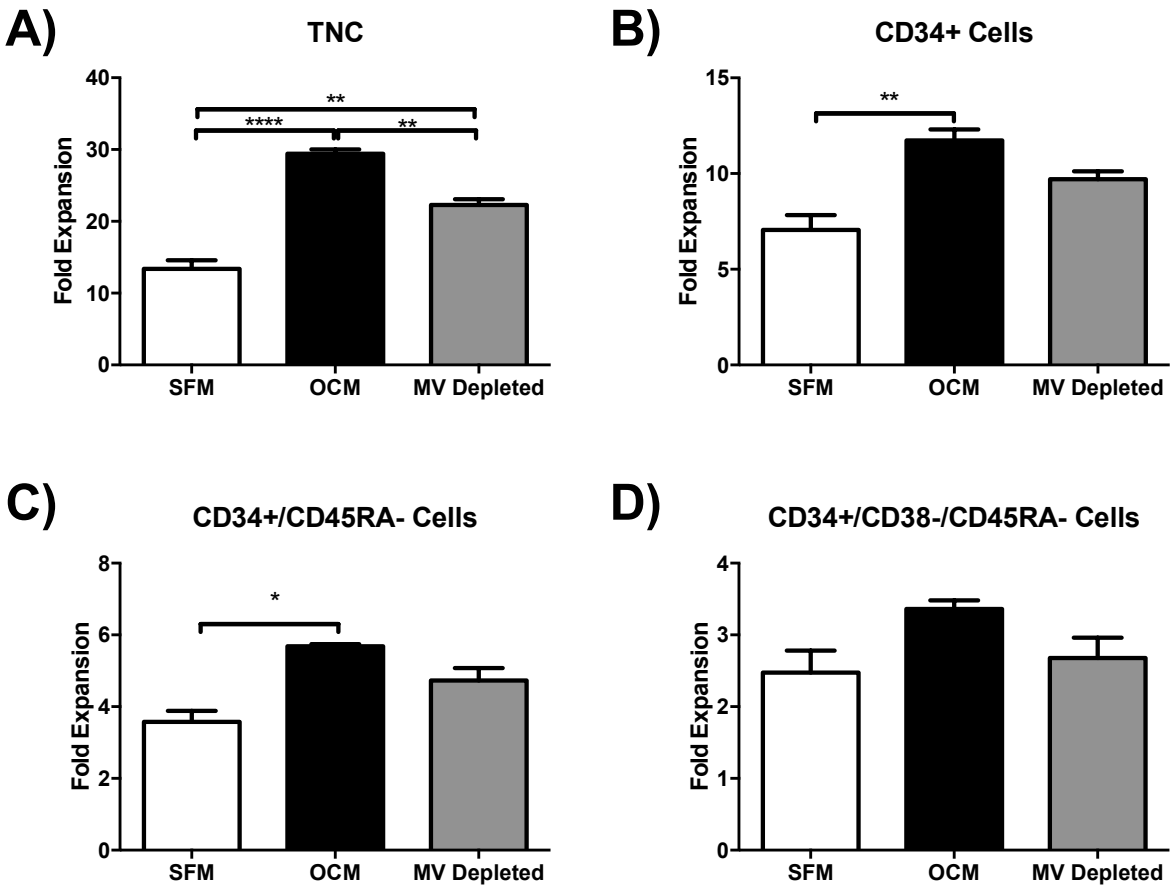

Figure 15: Impact of microparticle depletion on the growth activities of osteoblast conditioned media.

Panels A-D present the fold expansion in TNC, CD34+, CD34+CD45RA- and CD34+CD38-CD45RA- cells. Conditioned media was centrifuged at 20,000g for 30 minutes twice to remove microvesicle sized particles. Mean±SEM, n=3-5, ANOVA; * $p<0.05$, ** $p<0.01$, **** $p<0.0001$.

Chapter 4: Discussion

The osteogenesis of HSPCs leads to an increase in secretion of multiple factors. Some had already been implicated as regulators of HSPCs while others have yet to be characterized. I analyzed the secretome of immature osteoblasts in a biologically relevant method that leads to the expansion of HSPCs, and that has previously been associated with improved platelet engraftment[45]. In all, I identified 319 proteins, of which 47 were differentially expressed between HSPCs and osteoblasts (Figure 5; Table 3). The next stage of this osteoblast conditioned media project is to match the properties of osteoblast conditioned media with the secreted proteins that elicit the effect. After quantification of the secretome, our study started to characterize properties of identified proteins starting with SPARC which promoted the growth of CD34+ subpopulation. I showed the presence of extracellular vesicles in osteoblast conditioned media and showed that reduction of these extracellular vesicles reduces the growth promoting activity of osteoblast conditioned media.

4.1 Effects of secreted proteins from immature osteoblasts on HSPCs

There was an expectation for enrichment for biological processes such as ossification and extracellular matrix organization (Figure 8). There was enrichment for biological processes such as the complement pathway and cellular protein metabolic process (Figure 8). The complement proteins that I found upregulated in the secretome included C3, C1R, C1S, CFD and CFH, and I validated these through gene expression (Figure 10). The C3a fragment has been shown to improve homing HSPCs and in a phase 1 clinical trial improved platelet recovery slightly [96,97]. The other complement factor identified here has not been studied in *ex vivo* expansion of HSPCs and could

work synergistically or have individual effects on HSPCs. The contribution of these factors to the engraftment activity or growth promoting activity of osteoblast conditioned media will need further evaluation in subsequent studies.

The C3a fragment does not alter the expression of CXCR4 but primes SDF-1 interaction with CXCR4 promoting the interaction between VCAM-1 and VLA-4 [97]. VCAM-1 was found to be present in secretome and is known to change CD11a from its inactive form to active [98]. Both these factors have been shown to promote migration of HSPCs. Osteoblast conditioned media has been shown to promote both the migration and increased expression of some homing factors including CXCR4 [45] (Abu-Khader et al., Manuscript Submitted). The improved migration could be accounted for by these two factors, but other factor(s) likely contributes to increased expression of CXCR4. Synergistic effects between C3a and VCAM-1 have yet to be studied.

Another factor of interest yet to be tested is CD109 which promotes cell survival and osteoclast development [83,99]. CD109 promotes cell survival and proliferation through impairing TGFβ/SMAD-2/3 signalling, which has been shown in hepatocytes, HaLa, MCF-7 and MEL-28 cells [83]. Osteoclasts are derived from CD14+ monocytes which is a marker that increases in CD34+ cells grown in osteoblast conditioned media. CD109 promotes the differentiation of osteoclastogenesis from monocytes[99,100].

The “cellular protein metabolic process” is a biological process which includes C3, FSTL3, GAS6, IGF2, IGFBP2, IGFBP4, MXRA8 (Figure 8). All of these proteins have been shown to be involved with hematopoiesis, other than MXRA8 and IGFBP4. There was a correlation found between IGFBP4 expressing cells and hematopoiesis promoting activity, but this has not been followed up on [101]. FSTL3 enhances the

adhesion of fibronectin-1 to HSPCs [102]. While GAS6 maintains the number of CFC in culture in the absence of SCF [84]. IGF2 in murine models promotes the expansion of CFC-GEMM colonies and improves translation through regulation of the cell cycle [103]. Recent work by the Pineault lab showed that inhibition of IGF1R reduces the expansion of total nucleated cells and HSPC populations mediated by osteoblast conditioned media (Abu-Khader et al., Manuscript Submitted). While IGFBP2 expands HSPCs independent of IGF mechanisms through either synergy with NT-3 or Angptl5 [104,105]. The synergistic effect of IGFBP2 and Angptl5 not only has been shown to improve expansion but also engraftment. Investigation of IGFBP4's and MXRA8's effect on HSPCs, and if the proteins involved in "cellular protein metabolic process" biological process could work synergistically with each other. There is significant donor variation in the ability for dexamethasone to induce osteogenic differentiation of HSPCs, and this is potentially where some of the variations in principal component 2 are observed [106].

Our comparison between the differentially regulated proteins from our study and, Kim et al, 2012 and Kristensen et al, 2012, indicates the serum-free media that I use for conditioning stimulates pathways for insulin-like growth factor activity, integrin cell surface interactors and complement pathway (Figure 9). Other difference between our study and theirs that could contribute to different results included the mass spectrometer used, the quantification method and the cell donors. The other two studied have a similar conditioning process as our NO BIT treatment. Hence, it is tempting to hypothesize that one or the combination of these pathways could be involved in promote the expansion of HSPC with high thrombopoietic activity.

4.2 Effects of SPARC on HSPCs

One of the most exciting aspects of osteoblast conditioned media is its capacity to raise the thrombopoietic activity the expanded HSPC. SPARC knockouts in murine models lead to platelet deficiencies and reduced BFU-E colony forming cells [91]. It is believed that the improved platelet engraftment is in part due to the increased expansion of committed and multipotent progenitors [45,72]. Our study showed that SPARC promoted the expansion of CD34+CD45RA- and MPP populations but the mechanism by which SPARC acts on these populations is unknown (Figure 12). SPARC has multiple binding partners including, PDGFA, PDGFB, COL1A1 THBS1, VEGFA, FN1, TGFβ1, CD105, Integrin family proteins and ALB [107–111]

Stromal cell S17 maintains HSPCs independently from SCF interactions with its receptor c-kit, indicating other cytokines support HSCs through the same receptor [112]. Though SCF is well established as important to the maintenance of HSCs, other uncharacterized molecules could have overlapping functions. The SPARC Ca^{2+}-binding domain binds to VEGF-A on its VEGFR1 binding site and promotes VEGF-A binding to VEGFR2 [107,109]. VEGF-A is a factor that acts on HSCs in an autocrine fashion [113]. Dimerization of VEGFR2 maintains HSPCs independent of SCF [114]. Osteoblast conditioned media promoted hematopoietic stem and progenitor cell survival independently of SCF, but also synergized with SCF to promote cell growth (Abu-Khader et al., Manuscript Submitted).

One of SPARC's interacting partners is endoglin, a marker reported in human HSCs [109,115]. SPARC promotes the migration of pericytes through interactions to endoglin (CD105), a marker reported on HSCs. The interaction of SPARC and endoglin promote pericyte migration, therefore SPARC could affect the migration of HSPCs.

Investigation of how SPARC effects the erythroid and platelet lineages should be explored further. Colony forming cell assay would be required here to elucidate further how SPARC is affecting HSPCs. Based on the information stated above, the homing of HSPCs with SPARC should also be evaluated based on its interactions with endoglin and integrin proteins. Further investigation of SPARC's role in human hematopoiesis is required to understand how SPARC can be used in *ex vivo* expansion of human HSPCs.

4.3 Involvement of extracellular vesicles in HSPC growth

Force filtration has been implicated in causing deformation and breakup of larger extracellular particles [116]. Previous studies by Pineault laboratory used force filtration (0.2um) on osteoblast conditioned media, which caused the partial abolishment of the growth promoting effects on total nucleated and hematopoietic stem and progenitor cells and reduces platelet recovery [45,73]. The filtration results are consistent with depletion through centrifugation of extracellular vesicles (Figure 15) [73]. Force filtration did not have any effect on osteoblast conditioned media in the growth of CD14+ and CD41+ populations indicating that the soluble fraction likely works on these populations and this should be investigated to verify if this trend holds with CD14 and CD41 populations.

FASP columns have been shown as a method for isolating extracellular vesicles of exosomes and larger particles are held in the retentate. The activity of osteoblast conditioned media was retained within the retentate in all FASP column sizes tested (Figure 1). Combining the FASP column and force filtration data along with the overlap

of secretome proteins with microvesicles, the likelihood of large extracellular vesicles involved in the growth modulating activity of osteoblast condition media is quite high.

Using microvesicle isolation protocol, extracellular vesicles that were Annexin V+ with a median peak size of 132.9nm±8.1 were isolated (Figure 14). These extracellular vesicles that I isolated here fit both the criteria for microvesicles and matrix vesicles. The Annexin family of proteins have collagen binding properties and this family of proteins present on the surface of both microvesicles and matrix vesicles [117]. Treatments of collagenases improve the yield of matrix vesicles and could potentially improve yields of extracellular vesicles secreted by our immature osteoblasts [70]. The identification of the specific population of extracellular vesicles involved in the growth modulation of HSPCs will improve our understanding of their mechanism.

Attempts have been made at adding isolated extracellular vesicles from osteoblasts to CD34+ cultures, but thus far no changes in activity has been seen in these cultures. It is possible that the method of isolation may have affected the quality of the microvesicle-like particles; therefore, different methods of isolation may need to be explored. Though optimization on the number of extracellular vesicles required to be added to the culture and if the isolation method is affecting the integrity of the microvesicle-like particles still needs to be investigated.

Galectin-3, one of the proteins upregulated in the immature osteoblast secretome, had an adverse effect when the recombinant protein was added to HSPC cultures (Figure 9). While galectin-3 is secreted to signal extracellularly, galectin-3 can also be found in extracellular vesicles and transported intracellularly [118]. Galectin-3 containing extracellular vesicles have been associated with ALP activity similar to matrix vesicles.

Additionally, these vesicles prevent β-catenin degradation in osteoblasts and may have a similar effect on β-catenin in HSPCs. Osteoblast conditioned media has been shown to increase β-catenin expression in CD34+ cells, galectin-3 delivered by extracellular vesicle could be one possible mechanism for this (Law, K., Unpublished). The effects of galectin-3 on HSPCs may be different from the recombinant protein if present in microvesicles and transported intracellularly into the hematopoietic progenitors.

Detection of extracellular vesicles is improved by using a shorter wavelength in the side scatter parameter [119]. The flow cytometer I used had a side scatter on the 633nm laser (Original Attune Flow Cytometer, Blue/Red configuration, Applied Biosystems). Only the largest particles going through our flow cytometer are likely being detected. Future characterization of these extracellular vesicles should be performed with a flow cytometer with a 405nm side scatter channel.

The first step in future work is to improve yields of extracellular vesicles and isolate functional extracellular vesicles through either a combination of collagenase or tangential flow filtration [120]. Further experiments will be required to confirm the contents of protein and RNA, and what function they have on the growth and differentiation of HSPCs in culture. Dividing the growth modulatory effects of osteoblast conditioned media between the soluble fraction and extracellular will help guide the matching up of effects and factors. Based on this data the important thrombopoietic activity likely comes from extracellular vesicles of the osteoblast conditioned media.

4.4 Future improvement of this study

Our study shows a wide range of proteins both secreted by immature osteoblasts and upregulated during osteogenesis. Some proteins not detected in this study have

been detected by other methods [45,72]. The dynamic range of the mass spectrometer is likely the limiting factor here and why other proteins were not detected. For future studies, if a deeper coverage of the secretome is required, fractionation of the peptides using either strong cation exchange, peptide isoelectric focusing, reverse-phase chromatography or a combination of these approaches should be used. Additionally, separating the soluble fraction of proteins from the extracellular vesicle would give a better understanding of the origin of each protein. The validation should be done at the protein level with either ELISA or western blotting as gene expression does not always follow the protein level.

Understanding what stimulates the osteoblasts to secrete the growth modulatory effects could allow a method that requires fewer manipulations than the CHASE method that I used. Individual testing of BIT components did not lead to secretion of growth modulating effects. StemCell Technologies notes in their data sheet that their BSA is screened for their ability to support optimal growth of human hematopoietic progenitor cells. I only tested one batch of BSA for its growth promoting effects. BSA is a non-homogenous mixture of proteins and responsible proteins required for secretion of growth modulating effects and assists in the understanding between immature osteoblast and HSPCs. The non-CHASEd conditioned media presented some bovine-specific peptides other than albumin that included HPX, ORM1, AFP, C3, CFB, C4, CXCL4, COL3A1 and HGFAC, all of which may have stimulatory effects on the osteoblasts.

4.5 Conclusions

When limited cell numbers are collected, the use of osteoblast conditioned media to increase cell numbers in umbilical cord or autologous transplants has great potential [1]. I have identified many factors secreted by osteoblasts that will need future study for their potential modulatory effects on HSPCs. I presented initial evidence for the involvement of extracellular vesicles, and further work is needed. This study has opened many avenues for future research.

References

1. Jingjing, X. & ChengCheng, Z. Ex vivo expansion of hematopoietic stem cells. *Sci. China Life Sci.* **58,** 839–853 (2015).
2. Brummendorf, T. H., Dragowska, W., Zijlmans, J. M. J. M., Thornbury, G. & Lansdorp, P. M. Asymmetric cell divisions sustain long-term hematopoiesis from single- sorted human fetal liver cells. *J. Exp. Med.* **188,** 1117–1124 (1998).
3. Beckmann, J., Scheitza, S., Wernet, P., Fischer, J. C. & Giebel, B. Asymmetric cell division within the human hematopoietic stem and progenitor cell compartment : identification of asymmetrically segregating proteins. *Cell* **109,** 5494–5501 (2007).
4. Seita, Jun; Weissman, I. L. Hematopoietic Stem Cell: Self-renewal versus Differentiation. *Wiley Interdiscip Rev Syst Biol Med* **2,** 640–653 (2010).
5. Sidney, L. E., Branch, M. J., Dunphy, S. E., Dua, H. S. & Hopkinson, A. Concise review: Evidence for CD34 as a common marker for diverse progenitors. *Stem Cells* **32,** 1380–1389 (2014).
6. Civin, C. I. *et al.* Antigenic analysis of hematopoiesis . III . A hematopoietic progenitor cell surface antigen defined by a monoclonal antibody raised against KG-1a cells . Information about subscribing to The Journal of Immunology is online at : . A Hematopoietic Progenito. (1984).
7. Bhatia, M., Bonnet, D., Murdoch, B., Gan, O. I. & Dick, J. E. A newly discovered class of human hematopoietic cells with SCID-repopulating activity. *Nat. Med.* **4,** 1038–1045 (1998).
8. Craig, W., Poppema, S., Little, M. T., Dragowska, W. & Lansdorp, P. M. CD45 isoform expression on human haemopoietic cells at different stages of development. *Br J Haematol* **88,** 24–30 (1994).
9. Attar, A. Changes in the Cell Surface Markers During Normal Hematopoiesis: A Guide to Cell Isolation. *Glob. J. Hematol. Blood Transfus.* **1,** 20–28 (2014).
10. Sawai, C. M. *et al.* Hematopoietic Stem Cells Are the Major Source of Multilineage Hematopoiesis in Adult Animals. *Immunity* **45,** 597–609 (2016).
11. Notta, F. *et al.* Distinct routes of lineage development reshape the human blood hierarchy across ontogeny. *Science (80-.).* **351,** (2016).
12. Doulatov, S., Notta, F., Laurenti, E. & Dick, J. E. Hematopoiesis: A human perspective. *Cell Stem Cell* **10,** 120–136 (2012).
13. Sarma, N. J., Takeda, A. & Yaseen, N. R. Colony Forming Cell (CFC) Assay for Human Hematopoietic Cells. *J. Vis. Exp.* 3–7 (2010). doi:10.3791/2195
14. Copelan, E. A. Hematopoietic Stem-Cell Transplantation. 1813–1826 (2006). doi:10.1056/NEJMra052638
15. Atkins, H. L. *et al.* Immunoablation and autologous haemopoietic stem-cell transplantation for aggressive multiple sclerosis: a multicentre single-group phase 2 trial. *Lancet* **388,** 576–585 (2016).
16. Miller, P. H., Knapp, D. J. H. F. & Eaves, C. J. Heterogeneity in hematopoietic stem cell populations: Implications for transplantation. *Curr. Opin. Hematol.* **20,** 257–264 (2013).
17. Wang, J. C., Doedens, M. & Dick, J. E. Primitive human hematopoietic cells are

enriched in cord blood compared with adult bone marrow or mobilized peripheral blood as measured by the quantitative in vivo SCID-repopulating cell assay. *Blood* **89,** 3919–3924 (1997).
18. Oran, B. & Shpall, E. Umbilical cord blood transplantation: a maturing technology. *Hematology Am. Soc. Hematol. Educ. Program* **2012,** 215–22 (2012).
19. Barker, J., Weisdorf, D. & Wagner, J. Creation of a Double Chimera after the Transplantation of Umbilical-Cord Blood from Two Partially Matched Unrelated Donors. *N. Engl. J. Med.* **344,** 1870–1871 (2001).
20. Barker, J. N. *et al.* Transplantation of 2 partially HLA-matched umbilical cord blood units to enhance engraftment in adults with hematologic malignancy. *Blood* **105,** 1343–1347 (2005).
21. Brunstein, C. G. *et al.* Allogeneic hematopoietic cell transplantation for hematologic malignancy: Relative risks and benefits of double umbilical cord blood. *Blood* **116,** 4693–4700 (2010).
22. Sideri, A. *et al.* An overview of the progress on double umbilical cord blood transplantation. *Haematologica* **96,** 1213–1220 (2011).
23. Gluckman, E. *et al.* Hematopoietic reconstitution in a patient with Fanconi's anemia by means of umbilical-cord blood from an HLA-identical sibling. *Cell. Ther. Transplant.* **2,** 1174–1178 (1989).
24. Uchida, N. *et al.* High doses of purified stem cells cause early hematopoietic recovery in syngeneic and allogeneic hosts. *J. Clin. Invest.* **101,** 961–966 (1998).
25. Pineault, N. *et al.* Individual and synergistic cytokine effects controlling the expansion of cord blood CD34+cells and megakaryocyte progenitors in culture. *Cytotherapy* **13,** 467–480 (2011).
26. Mendelson, A. & Frenette, P. S. Hematopoietic stem cell niche maintenance during homeostasis and regeneration. *Nat. Med.* **20,** 833–846 (2014).
27. Sotnezova, E. V., Andreeva, E. R., Grigoriev, A. I. & Buravkova, L. B. Ex Vivo Expansion of Hematopoietic Stem and Progenitor Cells from Umbilical Cord Blood. *Acta Naturae* **8,** 6–16 (2016).
28. Wagner, J. E. *et al.* Phase I/II Trial of StemRegenin-1 Expanded Umbilical Cord Blood Hematopoietic Stem Cells Supports Testing as a Stand-Alone Graft. *Cell Stem Cell* **18,** 144–155 (2016).
29. Morrison, S. J. & Scadden, D. T. The bone marrow niche for haematopoietic stem cells. *Nature* **505,** 327–334 (2014).
30. Acar, M. *et al.* Deep imaging of bone marrow shows non-dividing stem cells are mainly perisinusoidal. *Nature* **526,** 126–130 (2015).
31. Kunisaki, Y. *et al.* Arteriolar niches maintain haematopoietic stem cell quiescence. *Nature* **502,** 637–643 (2013).
32. Lo Celso, C. *et al.* Live-animal tracking of individual haematopoietic stem/progenitor cells in their niche. *Nature* **457,** 92–96 (2009).
33. Hu, X. *et al.* Identification of a common mesenchymal stromal progenitor for the adult haematopoietic niche. *Nat. Commun.* **7,** 1–14 (2016).
34. Adler, B. J., Kaushansky, K. & Rubin, C. T. Obesity-driven disruption of haematopoiesis and the bone marrow niche. *Nat. Rev. Endocrinol.* **10,** 737–748 (2014).
35. Chan, M. E., Adler, B. J., Green, D. E. & Rubin, C. T. Bone structure and B-cell

populations, crippled by obesity, are partially rescued by brief daily exposure to low-magnitude mechanical signals. *FASEB J.* **26,** 4855–4863 (2012).
36. Bilwani, F. A. & Knight, K. L. Adipocyte-Derived Soluble Factor(s) Inhibits Early Stages of B Lymphopoiesis. *J. Immunol.* **189,** 4379–4386 (2012).
37. Naveiras, O. *et al.* Bone-marrow adipocytes as negative regulators of the haematopoietic microenvironment. *Nature* **460,** 259–263 (2009).
38. Greenbaum, A. *et al.* CXCL12 in early mesenchymal progenitors is required for haematopoietic stem-cell maintenance. *Nature* **495,** 227–230 (2013).
39. Ding, L., Saunders, T. L., Enikolopov, G. & Morrison, S. J. Endothelial and perivascular cells maintain haematopoietic stem cells. *Nature* **481,** 457–462 (2012).
40. Lavoie, J. R. & Rosu-Myles, M. Uncovering the secretes of mesenchymal stem cells. *Biochimie* **95,** 2212–2221 (2013).
41. Friedenstein, A. J., Chailakhyan, R. K., Latsinik, N. V., Panasyuk, A. F. & Keiliss-Borok, I. V. *STROMAL CELLS RESPONSIBLE FOR TRANSFERRING THE MICROENVIRONMENT OF THE HEMOPOIETIC TISSUES*. *Transplantation* (1974). doi:10.1097/00007890-197404000-00001
42. Wang, H.-S. *et al.* Mesenchymal Stem Cells in the Wharton's Jelly of the Human Umbilical Cord. *Stem Cells* **22,** 1330–1337 (2004).
43. Zuk, P. A. *et al.* Human Adipose Tissue Is a Source of Multipotent Stem Cells. *Mol. Biol. Cell* **14,** 2372–2384 (2002).
44. Dominici, M. *et al.* Minimal criteria for defining multipotent mesenchymal stromal cells. The International Society for Cellular Therapy position statement. *Cytotherapy* **8,** 315–317 (2006).
45. Dumont, N. *et al.* Medium conditioned with mesenchymal stromal cell-derived osteoblasts improves the expansion and engraftment properties of cord blood progenitors. *Exp. Hematol.* **42,** 741–752 (2014).
46. Li, N. *et al.* Human mesenchymal stem cells improve ex vivo expansion of adult human CD34+peripheral blood progenitor cells and decrease their allostimulatory capacity. *Exp. Hematol.* **35,** 507–515 (2007).
47. Hammoud, M. *et al.* Combination of low O_2 concentration and mesenchymal stromal cells during culture of cord blood $CD34^+$ cells improves the maintenance and proliferative capacity of hematopoietic stem cells. *J. Cell. Physiol.* **227,** 2750–2758 (2012).
48. Walenda, T. *et al.* Synergistic effects of growth factors and mesenchymal stromal cells for expansion of hematopoietic stem and progenitor cells. *Exp. Hematol.* **39,** 617–628 (2011).
49. Bernardo, M. E. *et al.* Co-infusion of ex vivo-expanded, parental MSCs prevents life-threatening acute GVHD, but does not reduce the risk of graft failure in pediatric patients undergoing allogeneic umbilical cord blood transplantation. *Bone Marrow Transplant.* **46,** 200–207 (2011).
50. de Lima, M. *et al.* Cord-Blood Engraftment with Ex Vivo Mesenchymal-Cell Coculture. *N. Engl. J. Med.* **367,** 2305–2315 (2012).
51. Feng, X. & McDonald, J. M. Disorders of Bone Remodeling. *Annu. Rev. Pathol. Mech. Dis.* **6,** 121–145 (2011).
52. Zaidi, M. Skeletal remodeling in health and disease. *Nat. Med.* (2007). doi:10.1038/nm1593

53. Youssef, A., Aboalola, D. & Han, V. K. M. The Roles of Insulin-Like Growth Factors in Mesenchymal Stem Cell Niche. *Stem Cells Int.* **2017,** 1–12 (2017).
54. Rutkovskiy, A., Stensløkken, K.-O. & Vaage, I. J. Osteoblast Differentiation at a Glance. *Med. Sci. Monit. Basic Res.* **22,** 95–106 (2016).
55. Stein, G. S. *et al.* Runx2 control of organization, assembly and activity of the regulatory machinery for skeletal gene expression. *Oncogene* **23,** 4315–4329 (2004).
56. Langenbach, F. & Handschel, J. Effects of dexamethasone, ascorbic acid and β-glycerophosphate on the osteogenic differentiation of stem cells in vitro. *Stem Cell Res. Ther.* **17,** 423–430 (2013).
57. Xing, W. *et al.* Nuclear factor-E2-related factor-1 mediates ascorbic acid induction of osterix expression via interaction with antioxidant-responsive element in bone cells. *J. Biol. Chem.* **282,** 22052–22061 (2007).
58. Ahmed, N., Khokher, M. a & Hassan, H. T. Cytokine-induced expansion of human CD34+ stem/progenitor and CD34+CD41+ early megakaryocytic marrow cells cultured on normal osteoblasts. *Stem Cells* **17,** 92–99 (1999).
59. Jung, Y. *et al.* Cell-to-cell contact is critical for the survival of hematopoietic progenitor cells on osteoblasts. *Cytokine* **32,** 155–162 (2005).
60. Chitteti, B. R. *et al.* Osteoblast lineage cells expressing high levels of Runx2 enhance hematopoietic progenitor cell proliferation and function. *J. Cell. Biochem.* **111,** 284–294 (2010).
61. Mishima, S. *et al.* Effective ex vivo expansion of hematopoietic stem cells using osteoblast-differentiated mesenchymal stem cells is CXCL12 dependent. *Eur. J. Haematol.* **84,** 538–546 (2010).
62. Tiwari, A. *et al.* Ex vivo expansion of haematopoietic stem/progenitor cells from human umbilical cord blood on acellular scaffolds prepared from MS-5 stromal cell line. *J. Tissue Eng. Regen. Med.* **4,** 524–531 (2013).
63. Cocucci, E. & Meldolesi, J. Ectosomes and exosomes: Shedding the confusion between extracellular vesicles. *Trends Cell Biol.* **25,** 364–372 (2015).
64. Akers, J. C., Gonda, D., Kim, R., Carter, B. S. & Chen, C. C. Biogenesis of extracellular vesicles (EV): Exosomes, microvesicles, retrovirus-like vesicles, and apoptotic bodies. *J. Neurooncol.* **113,** 1–11 (2013).
65. Raposo, G. & Stoorvogel, W. Extracellular vesicles: Exosomes, microvesicles, and friends. *J. Cell Biol.* **200,** 373–383 (2013).
66. Burger, D. *et al.* High glucose increases the formation and pro-oxidative activity of endothelial microparticles. *Diabetologia* **60,** 1791–1800 (2017).
67. Xie, H. *et al.* Mesenchymal stem cell-derived microvesicles support Ex vivo expansion of cord blood-derived CD34+ cells. *Stem Cells Int.* **2016,** (2016).
68. Deng, L. *et al.* Osteoblast-derived microvesicles: A novel mechanism for communication between osteoblasts and osteoclasts. *Bone* **79,** 37–42 (2015).
69. Bottini, M. *et al.* Matrix vesicles from chondrocytes and osteoblasts: Their biogenesis, properties, functions and biomimetic models. *Biochim. Biophys. Acta - Gen. Subj.* **1862,** 532–546 (2018).
70. Balcerzak, M. *et al.* A comparative analysis of strategies for isolation of matrix vesicles. *Anal. Biochem.* **361,** 176–182 (2007).
71. Çelebi, B., Mantovani, D. & Pineault, N. Irradiated mesenchymal stem cells improve the ex vivo expansion of hematopoietic progenitors by partly mimicking the bone

marrow endosteal environment. *J. Immunol. Methods* **370,** 93–103 (2011).
72. Alsheikh, M., Abu-Khader, A., Michalicka, M., Pasha, R. & Pineault, N. Impact of osteoblast maturation on their paracrine growth enhancing activity on cord blood progenitors. *Eur. J. Haematol.* **98,** 542–552 (2017).
73. Abu-Khader, A., Pasha, R., Ward, G. C. D., Boisjoli, G. & Pineault, N. Characterization of the growth modulatory activities of osteoblast conditioned media on cord blood progenitor cells. *Cytotechnology* **68,** 2257–2269 (2016).
74. Cox, J. & Mann, M. MaxQuant enables high peptide identification rates, individualized p.p.b.-range mass accuracies and proteome-wide protein quantification. *Nat. Biotechnol.* **26,** 1367–1372 (2008).
75. Cox, J. *et al.* Accurate Proteome-wide Label-free Quantification by Delayed Normalization and Maximal Peptide Ratio Extraction, Termed MaxLFQ. *Mol. Cell. Proteomics* **13,** 2513–2526 (2014).
76. Tyanova, S. *et al.* The Perseus computational platform for comprehensive analysis of (prote)omics data. *Nat. Methods* **13,** 731–740 (2016).
77. Pathan, M. *et al.* FunRich: An open access standalone functional enrichment and interaction network analysis tool. *Proteomics* **15,** 2597–2601 (2015).
78. Pathan, M. *et al.* A novel community driven software for functional enrichment analysis of extracellular vesicles data. *J. Extracell. Vesicles* **6,** (2017).
79. Huggett, J. F. *et al.* The digital MIQE guidelines: Minimum information for publication of quantitative digital PCR experiments. *Clin. Chem.* **65,** 3605–3613 (2013).
80. Anderson, N. L. & Anderson, N. G. The Human Plasma Proteome. *Mol. Cell. Proteomics* **1,** 845–867 (2002).
81. Gagarina, V., Carlberg, A. L., Pereira-Mouries, L. & Hall, D. J. Cartilage oligomeric matrix protein protects cells against death by elevating members of the IAP family of survival proteins. *J. Biol. Chem.* **283,** 648–659 (2008).
82. Neidhart, M. *et al.* Galectin-3 is induced in rheumatoid arthritis synovial fibroblasts after adhesion to cartilage oligomeric matrix protein. *Ann. Rheum. Dis.* **64,** 419–424 (2005).
83. Zong, G. *et al.* CD109 Mediates Cell Survival in Hepatocellular Carcinoma Cells. *Dig. Dis. Sci.* **61,** 2303–2314 (2016).
84. Dormady, S. P., Zhang, X.-M. & Basch, R. S. Hematopoietic progenitor cells grow on 3T3 fibroblast monolayers that overexpress growth arrest-specific gene-6 (GAS6). *Proc. Natl. Acad. Sci. U.S.A.* **97,** 12260–12265 (2000).
85. Park, I.-K. *et al.* The Axl / Gas6 pathway is required for optimal cytokine signaling during human natural killer cell development. *Blood* **113,** 2470–2477 (2009).
86. Dumic, J., Dabelic, S. & Flögel, M. Galectin-3: An open-ended story. *Biochim. Biophys. Acta - Gen. Subj.* **1760,** 616–635 (2006).
87. Shimura, T. *et al.* Galectin-3, a novel binding partner of beta-catenin. *Cancer Res.* **64,** 6363–6367 (2004).
88. Shimura, T. *et al.* Implication of Galectin-3 in Wnt Signaling Implication of Galectin-3 in Wnt Signaling. 3535–3537 (2005). doi:10.1158/0008-5472.CAN-05-0104
89. Eckfeldt, C. E. *et al.* Functional Analysis of Human Hematopoietic Stem Cell Gene Expression Using Zebrafish. *PLoS Biol.* **3,** e254 (2005).
90. Siva, K. *et al.* SPARC is dispensable for murine hematopoiesis, despite its suspected pathophysiological role in 5q-myelodysplastic syndrome. *Leukemia* **26,** 2416–2419

(2012).
91. Lehmann, S. *et al.* Common deleted genes in the 5q-syndrome: Thrombocytopenia and reduced erythroid colony formation in SPARC null mice. *Leukemia* **21,** 1931–1936 (2007).
92. Ehninger, A. *et al.* Loss of SPARC protects hematopoietic stem cells from chemotherapy toxicity by accelerating their return to quiescence. *Blood* **2,** 2320–2338 (2014).
93. Timari, H. *et al.* The effect of mesenchymal stem cell-derived extracellular vesicles on hematopoietic stem cells fate. *Adv. Pharm. Bull.* **7,** 531–546 (2017).
94. Akbar, N. *et al.* Endothelium-derived extracellular vesicles promote splenic monocyte mobilization in myocardial infarction. *JCI Insight* **2,** 1–17 (2017).
95. Andresen, T. K., Svennevig, J. L. & Videm, V. Soluble VCAM-1 is a very early marker of endothelial cell activation in cardiopulmonary bypass. *Perfusion* **17,** 15–21 (2002).
96. Brunstein, C. G. *et al.* Complement fragment 3a priming of umbilical cord blood progenitors: Safety profile. *Biol. Blood Marrow Transplant.* **19,** 1474–1479 (2013).
97. Reca, R. *et al.* Functional receptor for C3a anaphylatoxin is expressed by normal hematopoietic stem/progenitor cells, and C3a enhances their homing-related responses to SDF-1. *Blood* **101,** 3784–3793 (2003).
98. Perdomo-Arciniegas, A.-M. & Vernot, J.-P. Co-culture of hematopoietic stem cells with mesenchymal stem cells increases VCAM-1-dependent migration of primitive hematopoietic stem cells. *Int. J. Hematol.* **94,** 525–532 (2011).
99. Wang, Y., Inger, M., Jiang, H., Tenenbaum, H. & Glogauer, M. CD109 Plays a Role in Osteoclastogenesis. *PLoS One* **8,** (2013).
100. Massey, H. M. & Flanagan, A. M. Human osteoclasts derive from CD14-positive monocytes. *Br. J. Haematol.* **106,** 167–170 (1999).
101. Grellier, P., Yee, D., Gonzalez, M. & Abboud, S. L. Characterization of insulin-like growth factor binding proteins (IGFBP) and regulation of IGFBP-4 in bone marrow stromal cells. *Br J Haematol* **90,** 249–257 (1995).
102. Maguer-Satta, V. *et al.* A novel role for fibronectin type I domain in the regulation of human hematopoietic cell adhesiveness through binding to follistatin domains of FLRG and follistatin. *Exp. Cell Res.* **312,** 434–442 (2006).
103. Thomas, D. D. *et al.* Insulin-like growth factor 2 (IGF2) modulates murine hematopoietic stem cell maintenance through upregulation of p57. *Exp Hematol* **44,** 422–433 (2016).
104. Çelebi, B., Mantovani, D. & Pineault, N. Insulin-like growth factor binding protein-2 and neurotrophin 3 synergize together to promote the expansion of hematopoietic cells ex vivo. *Cytokine* **58,** 327–331 (2012).
105. Zhang, C. C., Kaba, M., Iizuka, S., Huynh, H. & Harvey, F. Angiopoietin-like 5 and IGFBP2 stimulate ex vivo expansion of human cord blood hematopoietic stem cells as assayed by NOD/SCID transplantation. *Hematology* **111,** 3415–3423 (2008).
106. Siddappa, R., Licht, R., van Blitterswijk, C. & de Boer, J. Donor variation and loss of multipotency during in vitro expansion of human mesenchymal stem cells for bone tissue engineering. *J. Orthop. Res.* **7,** 1029–1041 (2007).
107. Kupprion, C., Motamed, K. & Sage, E. H. SPARC (BM-40, osteonectin) inhibits the mitogenic effect of vascular endothelial growth factor on microvascular endothelial cells. *J. Biol. Chem.* **273,** 29635–29640 (1998).

108. Sage, H., Vernon, R. B., Funk, S. E., Everitt, E. A. & Angello, J. SPARC, a secreted protein associated with cellular proliferation, inhibits cell spreading in vitro and exhibits Ca+2-dependent binding to the extracellular matrix. *J. Cell Biol.* **109,** 341–356 (1989).
109. Rivera, L. B. & Brekken, R. A. SPARC promotes pericyte recruitment via inhibition of endoglin-dependent TGF-β1 activity. *J. Cell Biol.* **193,** 1305–1319 (2011).
110. Raines, E. W., Lane, T. F., Iruela-Arispe, M. L., Ross, R. & Sage, E. H. The extracellular glycoprotein SPARC interacts with platelet-derived growth factor (PDGF)-AB and -BB and inhibits the binding of PDGF to its receptors. *Proc. Natl. Acad. Sci. U. S. A.* **89,** 1281–1285 (1992).
111. Francki, A. *et al.* SPARC regulates TGF-beta1-dependent signaling in primary glomerular mesangial cells. *J. Cell. Biochem.* **91,** 915–925 (2004).
112. Wineman, J. P., Nishikawa, S. & Muller-Sieburg, C. E. Maintenance of High Levels of Pluripotent Hematopoietic Stem Cells In Vitro: Effect of Stromal Cells and c-kit. *Blood* **114,** 467–478 (1993).
113. Gerber, H. P. *et al.* VEGF regulates haematopoietic stem cell survival by an internal autocrine loop mechanism. *Nature* **417,** 954–958 (2002).
114. Larrivée, B. *et al.* Vascular endothelial growth factor receptor-2 induces survival of hematopoietic progenitor cells. *J. Biol. Chem.* **278,** 22006–13 (2003).
115. Pierelli, L. *et al.* CD105 (endoglin) expression on hematopoietic stem/progenitor cells. *Leuk. Lymphoma* **8194,** (2001).
116. Witwer, K. W. *et al.* Standardization of sample collection, isolation and analysis methods in extracellular vesicle research. *J. Extracell. Vesicles* **2,** 1–25 (2013).
117. Kirsch, T. & Pfaffle, M. Selective Binding of Anchorin-CII (Annexin-V) to Type-II and X-Collagen and to Chondrocalcin (C-Propeptide of Type-II Collagen) - Implications for Anchoring Function Between Matrix Vesicles and Matrix Proteins. *FEBS Lett.* **310,** 143–147 (1992).
118. Weilner, S. *et al.* Vesicular Galectin-3 levels decrease with donor age and contribute to the reduced osteo-inductive potential of human plasma derived extracellular vesicles. *Aging (Albany. NY).* **8,** 16–30 (2016).
119. McVey, M. J., Spring, C. M. & Kuebler, W. M. Improved resolution in extracellular vesicle populations using 405 instead of 488 nm side scatter. *J. Extracell. Vesicles* **7,** (2018).
120. Tan, C. *et al.* Mesenchymal stem cell-derived exosomes promote hepatic regeneration in drug-induced liver injury models. *Stem Cell Res. Ther.* **5,** 76 (2014).

Appendix

6.1 Evaluation of Wnt expression during osteoblast differenation

Previous work by Mathew Michelicka in the Pineault laboratory showed there is an involvement of β-catenin in coculture of day 6 osteoblasts and HSCs in the expansion of HSCs using the β-catenin/TCF iCRT3 inhibitor. With the abundance of publicly available "-omics" data, these datasets can be used to save both time and money, targeting experiments more efficiently. The BioGPS primary cell atlas was used for efficient screening of growth factors that target β-catenin. A comparison between HSPCs and day seven osteoblasts, from the primary cell atlas, was made by screening Wnt and other growth factors for an upregulation greater than a 1.2-fold increase. "Tissue_stemcells:bm_msc:cntrl.1" and "Tissue_stemcells:bm_msc:osteogenic_induction_7d.1" were compared identifying Wnt3 (1.5x), Wnt4 (1.8x), Wnt5a (1.2x), Wnt9a (1.2x), Wnt9b(1.4x) and Wnt10b(1.2x). From these genes, Wnt3, Wnt4 and Wnt5a were selected to follow up with using qPCR to assess if there was an upregulation of these genes in our system (Supplemental Figure 3). Using qPCR Wnt3 (1.9-fold increase, $p=0.043$) and Wnt4 (12.1-fold increase, $p=0.015$) showed a significant increase during differentiation while Wnt5a observed no significant change. Validation of Wnt3 and Wnt4 in our system identifies potential targets for further β-catenin targets for screening.

Screening of IGFBP2 (2.0x), IGF2 (8.4x) and CXCL1 (5.0x), which were previously validated and matched treads observed in BioGPS database. Additional genes were screened using this methodology and still require validation, these include

ANGPT1 (1.5x), ANGPT-L4 (1.6x), CXCL6 (4x), CXCL8 (2.4x), CXCL14 (1.6x), FGF6 (1.8x), FGF7 (2.2x), FGF17 (1.9x), FGF20 (1.6x), FGF21 (1.5x), IGFBP4 (1.6x), IL13 (1.4x), IL14 (1.4x) and IL16 (1.3x). These genes screened here could lead to additional targets for osteoblast activity on HSCs and additional projects for future students.

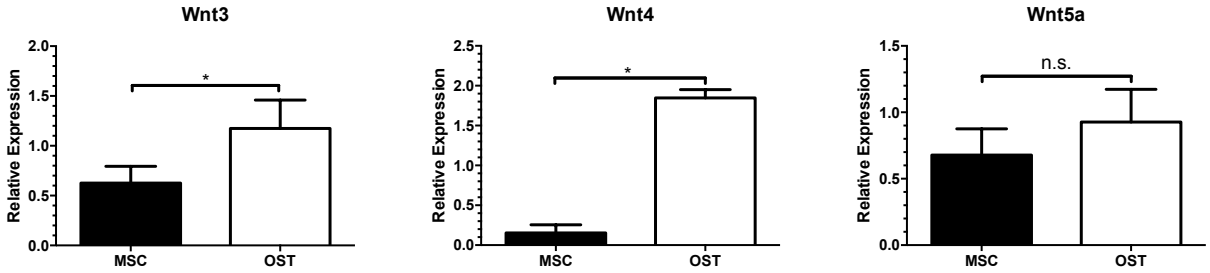

Supplemental Figure 1: Changes in Wingless-ints (Wnt) gene expression during osteogenic differentiation. Comparison of selected Wnt genes from BioGPS database. Comparing undifferentiated mesenchymal stem and day 6 osteoblast gene expression. Data used for Michelicka et al, 2017. n=3, paired t-test, * $p<0.05$